ResearchGate

See discussions, stats, and author profiles for this publication at: https://www.researchgate.net/publication/236915979

Complete Photochromic Structural Changes in Ruthenium(II)Diimine Complexes, Based on Control of the Excited States by Metalation

ARTICLE *in* CHEMISTRY - A EUROPEAN JOURNAL · JULY 2013

Impact Factor: 5.73 · DOI: 10.1002/chem.201300437 · Source: PubMed

CITATIONS
3

READS
33

6 AUTHORS, INCLUDING:

Tomoya Ishizuka
University of Tsukuba
58 PUBLICATIONS **1,268** CITATIONS
SEE PROFILE

Takahiko Kojima
University of Tsukuba
131 PUBLICATIONS **2,263** CITATIONS
SEE PROFILE

Available from: Takahiko Kojima
Retrieved on: 24 January 2016

CHEMISTRY
A EUROPEAN JOURNAL

ChemPubSoc Europe

DOI: 10.1002/chem.201300437

Complete Photochromic Structural Changes in Ruthenium(II)–Diimine Complexes, Based on Control of the Excited States by Metalation

Takuya Sawaki,[a] Tomoya Ishizuka,[a] Masaki Kawano,[b] Yoshihito Shiota,[c] Kazunari Yoshizawa,[c] and Takahiko Kojima*[a]

Abstract: The thermal and photochemical reactions of a newly synthesized complex, $[Ru^{II}(TPA)(tpphz)]^{2+}$ (**1**; TPA = tris(2-pyridylmethyl)amine, tpphz = tetrapyrido[3,2-*a*:2′,3′-*c*:3″,2″-*h*:2‴,3‴-*j*]phenazine), and its derivatives have been investigated. Heating a solution of complex **1** (closed form) and its derivatives in MeCN caused the partial dissociation of one pyridylmethyl moiety of the TPA ligand and the resulting vacant site on the Ru^{II} center was occupied by a molecule of MeCN from the solvent to give a dissociated complex, $[Ru^{II}(\eta^3\text{-TPA})(tpphz)(MeCN)]^{2+}$ (**1′**, open form), and its derivatives, respectively, in quantitative yields. The thermal dissociation reactions were investigated on the basis of kinetics analysis, which indicated that the reactions proceeded through a seven-coordinate transition state. Although the backwards reaction was induced by photoirradiation of the MLCT absorption bands, the photoreaction of complex **1′** reached a photostationary state between complexes **1** and **1′** and, hence, the recovery of complex **1** from complex **1′** was 67%. Upon protonation of complex **1** at the vacant site of the tpphz ligand, the efficiency of the photoinduced recovery of complex **1**+H^+ from complex **1′**+H^+ improved to 83%. In contrast, dinuclear μ-tpphz complexes **2** and **3**, which contained the $Ru^{II}(TPA)(tpphz)$ unit and either a $Ru^{II}(bpy)_2$ or $Pd^{II}Cl_2$ moiety on the other coordination edge of the tpphz ligand, exhibited 100% photoconversion from their open forms into their closed forms (**2′**→**2** and **3′**→**3**). These results are the first examples of the complete photochromic structural change of a transition-metal complex, as represented by complete interconversion between its open and closed forms. Scrutinization by performing optical and electrochemical measurements allowed us to propose a rationale for how metal coordination at the vacant site of the tpphz ligand improves the efficiency of photoconversion from the open form into the closed form. It is essential to lower the energy level of the triplet metal-to-ligand charge-transfer excited state (^{3}MLCT*) of the closed form relative to that of the triplet metal-centered excited state (^{3}MC*) by metal coordination. This energy-level manipulation hinders the transition from the ^{3}MLCT* state into the ^{3}MC* state in the closed form to block the partial photodissociation of the TPA ligand.

Keywords: kinetics · metalation · photochromism · reaction mechanisms · ruthenium

Introduction

Switchable molecular motions,[1] such as shuttling,[2] sliding,[3] rotation,[4–7] and tweezing,[8] have attracted considerable attention, owing to their relevance to natural biomachines, such as myosin in muscular tissue[1,9] and the F_1 unit of ATP synthase,[1,10] as well as for future applications in molecular machines.[11] Synthetic molecular machines can function by using, for example, acid/base reactions,[12] electrochemical redox processes,[13,14] photoinduced structural changes,[15] and chemical oxidation[16] as the driving force of the motion. These machines can function as molecular sensors,[17] elicit mechanical forces,[18] and perform as cooperative molecular catalysts.[19] Among the various molecular motions, capping/uncapping motions in molecules are expected to be useful for controlled molecular recognition and catalytic reaction systems, whose functions can be switched by using an external stimuli (Figure 1a).[20]

Reversible structural change in transition-metal complexes at metal centers are also attractive in light of the de-

[a] T. Sawaki, Dr. T. Ishizuka, Prof. Dr. T. Kojima
Department of Chemistry
Graduate School of Pure and Applied Sciences
University of Tsukuba
1-1-1 Tennoudai, Tsukuba, Ibaraki 305-8571 (Japan)
Fax: (+81) 29-825-6503
E-mail: kojima@chem.tsukuba.ac.jp

[b] Prof. Dr. M. Kawano
Division of Advanced Materials Science (WCU project)
Pohang University of Science and Technology (POSTECH)
San 31 Hyojadong, Pohang 790-784 (South Korea)

[c] Dr. Y. Shiota, Prof. Dr. K. Yoshizawa
Institute for Materials Chemistry and Engineering
Kyushu University
Motooka, Nishi-Ku, Fukuoka 819-0395 (Japan)

Supporting information for this article is available on the WWW under http://dx.doi.org/10.1002/chem.201300437.

WILEY ONLINE LIBRARY

© 2013 Wiley-VCH Verlag GmbH & Co. KGaA, Weinheim

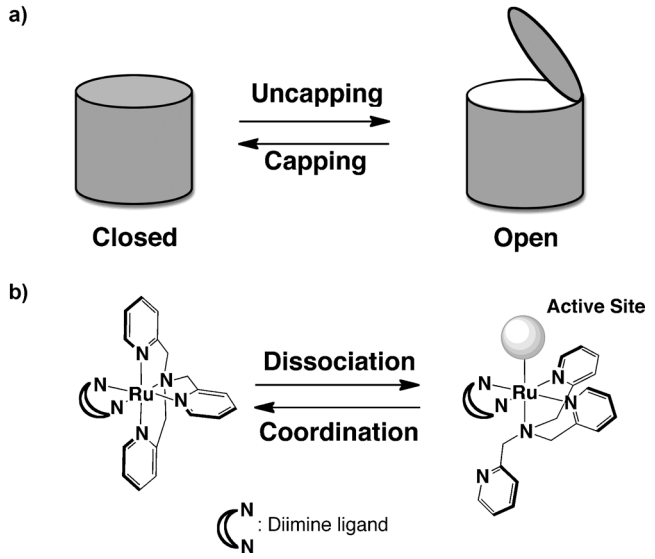

Figure 1. a) Schematic representation of the "capping/uncapping" motion and b) reversible dissociation/coordination of a Ru^{II}(TPA)(diimine) complex.

velopment of molecular machines and devices to perform various functionalities that are unique to metal complexes, including catalysis and the switching of their physical properties. Transition-metal complexes that respond to external stimuli have been reported to demonstrate reversible structural changes, including reversible ligand-coordination/dissociation owing to changes in pH value[21] and the translocation of metal ions through changes in pH value[22] and redox reactions.[23] As a photochemical response of transition-metal complexes, photochromic reactions, such as reversible structural changes that involve a partial dissociation and the recoordination of a ligand, have also been investigated.[24,25] In such a structural change, the vacant coordination site that is formed by the partial dissociation of the ligand can be used as a guest-binding or catalytically active site; thus, the dissociable part of the ligand plays a role as a "cap" for the active site. However, for transition-metal complexes, there have been no examples so far of completely reversible photochromic structural changes for attaining complete interconversion between two states without reaching a photostationary state. Recently, we reported reversible photochromic structural changes in Ru^{II}–tris(2-pyridylmethyl)amine (TPA) complexes that contained a diimine ligand, such as 2,2′-bipyridine (bpy), 2,2′-bipyrimidine (bpm), or 1,10-phenanthlorine (phen, Figure 1b).[26] However, the conversion efficiencies for the photochromic reactions of transition-metal complexes, including our previous examples, were not 100% and, in most cases, illumination of the photochromic complexes afforded a photostationary state between two states.[24–27]

Herein, we report the first examples of molecular bistability, which involve complete photochromic structural changes in new Ru^{II}–TPA complexes that contain tetrapyrido-[3,2-*a*:2′,3′-*c*:3″,2″-*h*:2″,3‴-*j*]phenazine (tpphz)[28] as a diimine ligand (Figure 2). The tpphz ligand is a highly planar and extensively π-conjugated heteroaromatic molecule. In addition, the tpphz ligand has another coordination site on the opposite side to the side that coordinates to the Ru^{II}(TPA) unit and we utilize this site to accept a H^+ ion (proton) or other transition-metal ions, such as Ru^{II} and Pd^{II} ions (Figure 2).[29] These kinds of additives can influence both the ground and excited electronic states, owing to their strong interactions with the diimine ligand in different manners. The influence of additives can regulate the dissociation/coordination reactions of the TPA ligand in the Ru^{II}(TPA) moiety to accomplish the complete interconversion between its open form, which contains a facial η^3-TPA ligand, and its closed form, which contains an η^4-TPA ligand, as shown in Figure 2.

Results and Discussion

Syntheses and structural characterization: 1,10-Phenanthroline-5,6-dione (phendione)[30] was coordinated to a Ru^{II}(TPA) complex to obtain $[Ru^{II}(TPA)(phendione)](PF_6)_2$. The phendione complex was coupled with 5,6-diamino-1,10-phenanthroline (phendiamine)[31] to construct the tpphz moiety (Scheme 1a). In the previous report of the synthesis of a Ru^{II}(tpphz) complex,[28] the solvent for the coupling reaction between a Ru^{II}(phendione) complex and phendiamine was MeCN. However, in our case, MeCN caused the dissociation of a pyridine moiety of the TPA ligand from Ru^{II}(TPA)(diimine) complexes.[26] Thus, we employed MeOH as the reaction solvent and the total yield of target complex $[Ru^{II}(TPA)(tpphz)](PF_6)_2$ (**1**) was 74% (over 2 steps). In addition, the protonated complex, $[Ru^{II}(TPA)(tpphz\text{-}H^+)](PF_6)_3$ ($[\mathbf{1}{+}H]^+$), was isolated by recrystallization from its solution in MeCN

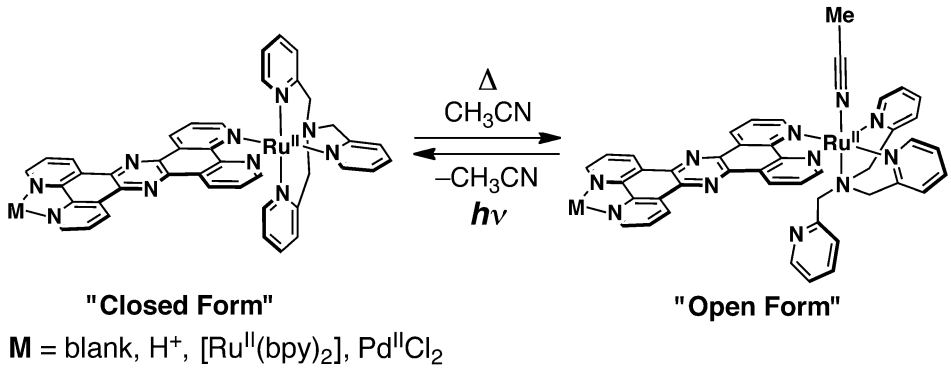

Figure 2. Interconversion between the "open" and "closed" forms in Ru^{II}(TPA)(tpphz) complexes.

 © 2013 Wiley-VCH Verlag GmbH & Co. KGaA, Weinheim

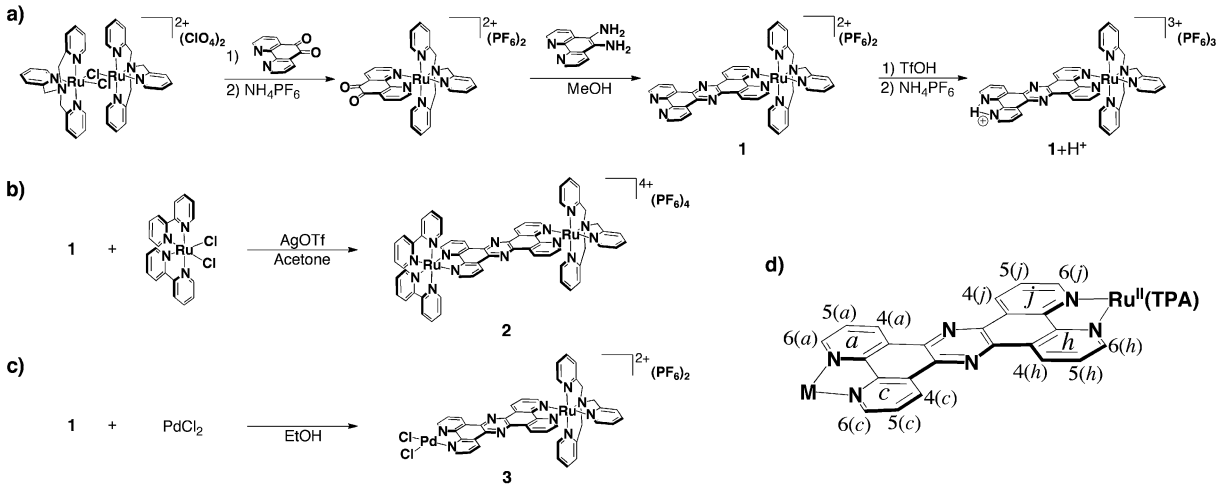

Scheme 1. Synthesis of Ru^{II}(TPA)(tpphz) complexes **1**, **1**+H^+, **2**, and **3** (a–c) and the labeling of the tpphz ligand for ^{1}H NMR assignment (d).

in the presence of trifluoromethanesulfonic acid (TfOH), in which EtOAc was used as a poor solvent. The protonation probably occurred at the vacant coordination site of the tpphz ligand and the central pyrazine moiety of the tpphz ligand could not be protonated under these conditions, because the imine nitrogen atom on the pyradine moiety was sterically hindered by the neighboring hydrogen atoms at the 4(*a*), 4(*c*), 4(*h*), and 4(*j*)-positions of the tpphz ligand.[28b]

$[Ru^{II}(bpy)_2(solv)_2](OTf)_2$ (bpy = 2,2′-bipyridine, solv = acetone) was prepared according to a literature procedure[32] and was ligated to the vacant coordination site of complex **1** in acetone, which was chosen as the solvent because of the weak coordinating ability without the pyridine-dissociation reaction of the Ru^{II}(TPA) unit.[26,33] After repeated recrystallization, a dinuclear tpphz complex, $[(bpy)_2Ru^{II}(\mu\text{-tpphz})Ru^{II}(TPA)](PF_6)_4$ (**2**), was obtained in 80% yield. A hetero-dinuclear complex, $[Cl_2Pd(\mu\text{-tpphz})Ru^{II}(TPA)](PF_6)_2$ (**3**), was synthesized through the coordination of $PdCl_2$ to the vacant site of complex **1** (Scheme 1c). Although we applied a literature procedure[29,34] to the synthesis of a $PdCl_2$–μ-tpphz–Ru^{II} complex, at first, our attempts were unsuccessful. The coordination reaction at high temperatures in DMF or ethyleneglycol caused the decomposition of the obtained product before completion of the reaction. Finally, we found that the reaction at reflux in EtOH was the best for obtaining the target Pd complex (**3**) and the reaction yield was 43% after isolation by repeated recrystallization.

Structural characterization of complexes **1**, [**1**+H]$^+$, **2**, and **3** was performed by using ^{1}H NMR spectroscopy and MS (ESI-TOF); complex **1** was also characterized by single-crystal X-ray diffraction (see below). Peak clusters that were ascribed to the mass signals of complexes $[\mathbf{1}-2PF_6]^{2+}$, $[\mathbf{2}-4PF_6]^{4+}$, and $[\mathbf{3}-2PF_6]^{2+}$ were observed at $m/z = 388.1$ as a dicationic signal with a 0.5 peak separation, $m/z = 297.6$ as a tetracationic signal with a 0.25 peak separation, and $m/z = 477.0$ as a dicationic signal with a 0.5 peak separation, respectively (Figure 3). The MS (ESI) spectrum of complex [**1**+H]$^+$ gave a peak cluster that was ascribed to deprotonated species $[\mathbf{1}-2PF_6]^{2+}$, presumably owing to deprotonation during the ionization process in the MS measurements.

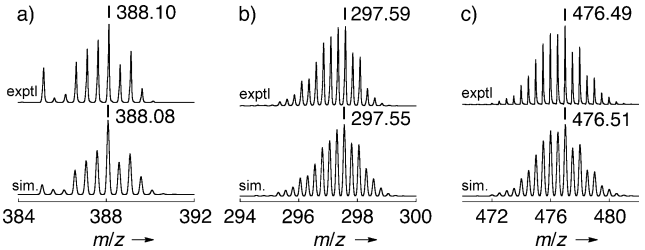

Figure 3. MS (ESI-TOF) spectra of complexes **1** (a), **2** (b), and **3** (c). Top: experimental results; bottom: simulated spectra.

In the ^{1}H NMR spectra of complexes **1**, [**1**+H]$^+$, **2**, and **3** in [D_3]MeCN (Figure 4 and the Supporting Information, Figures S1–S4), the ^{1}H NMR signals of the axial and the two equatorial pyridylmethyl moieties in the TPA ligand were inequivalent and the methylene signals of the equatorial pyridylmethyl moieties were observed at about $\delta = 4.5$ ppm as AB quartets with coupling constants of $J \approx 15$ Hz.[26,33,35,36] In all four complexes, the ^{1}H NMR signals of the pyridyl protons at the 6-position of the axial pyridine rings, which was the closest to the tpphz moieties, were downfield-shifted to about $\delta = 10$ ppm, owing to the deshielding effect from the ring current of the tpphz ligand (Figure 4). In addition, the ^{1}H NMR signal of the 6-proton on the *h*-pyridine ring in the tpphz ligand was also affected by the ring current of the axial pyridine rings and, hence, was also downfield-shifted. The chemical shift values of the 4(*h*), 4(*j*), 5(*j*), 6(*j*), and py-6(eq) protons in complexes **1**, [**1**+H]$^+$, and **3** were highly dependent on the concentration of the sample solutions (see the Supporting Information, Figure S5), whereas the UV/Vis spectra of these three complexes did not exhibit any concentration dependence. These ^{1}H NMR shifts can be ascribed to intermolecular π–π stacking interactions between the tpphz ligands, as previously reported for $[Ru^{II}(bpy)_2(tpphz)]^{2+}$.[28] In contrast, the ^{1}H NMR spectrum of complex **2** did not ex-

 © 2013 Wiley-VCH Verlag GmbH & Co. KGaA, Weinheim

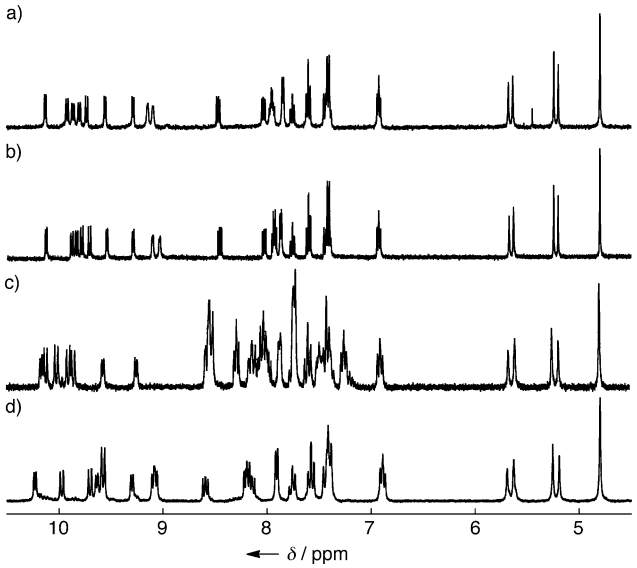

Figure 4. ^{1}H NMR spectra of complexes **1** (a), $[\mathbf{1}+H]^+$ (b), **2** (c), and **3** in $[D_3]$MeCN (d). Concentration: 1.7 mM (a), 1.6 mM (b), 1.3 mM (c), 1.5 mM (d).

hibit any concentration dependence. Two sets of pyridine signals for the bpy ligand in complex **2** were observed, which were assigned to the axial and equatorial pyridine moieties. The independence of the chemical shifts on the concentration of complex **2** should be derived from the steric congestion of the two bpy and the TPA ligands around the tpphz ligand. The bulkiness of the TPA ligand and the two bpy ligands at the Ru centers may prevent intermolecular π–π stacking of the tpphz ligands and, hence, our attempts at crystallization were unsuccessful.

The DFT-optimized structure of complex **2** indicates that the tpphz ligand maintains planarity (mean deviation from the plane of the tphz ligand: 0.021 Å) and causes tilting of one of the pyridine rings of the TPA ligand, owing to steric hindrance, as observed in other related Ru^{II}(TPA)(diimine) complexes (Figure 5).[26] The optimized structure of complex **2′** also has a slightly bent tpphz ligand (mean deviation from the plane of the tpphz ligand: 0.165 Å) and a tridentate TPA ligand, with one uncoordinated pyridylmethyl arm. The calculated energy of complex **2′** is $-78.9\ kJ\,mol^{-1}$ relative to that of complex **2**, with one accompanying free MeCN molecule. Thus, the binding energy of the MeCN ligand was roughly estimated. In addition, the inter-Ru distances were calculated to be 13.02 Å in complex **2** and 12.98 Å in complex **2′**. The LUMO and LUMO+1 resided on the tpphz ligand as π* orbitals. The HOMO was located on the Ru^{II} center of the Ru^{II}(TPA) unit and the HOMO−1 was located on the Ru^{II} center of the $Ru^{II}(bpy)_2$ unit (see the Supporting Information, Figure S6). The order of the energy levels indicates that the Ru^{II} center in the Ru^{II}(TPA) unit is more easily oxidized than that in the $Ru^{II}(bpy)_2$ unit. On the other hand, the relative positions of the HOMO and HOMO−1 were exchanged in complex **2′**: The HOMO was located on the Ru^{II} center of the $Ru^{III}(bpy)_2$ unit and the HOMO−1

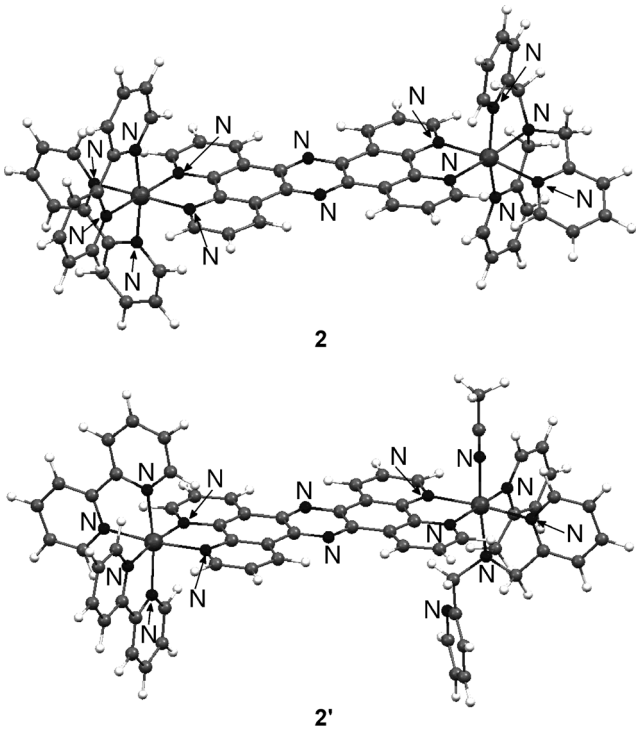

Figure 5. DFT-optimized structures of complexes **2** and **2′** at the B3LYP/SDD level of theory.

was located on the Ru^{II} center of the Ru^{II}(TPA) unit (see the Supporting Information, Figure S7). The relative positions of the LUMO and the LUMO+1 remained unchanged during the isomerization process.

Crystal structure of complex 1: Mononuclear complex **1** crystallized in the monoclinic space group $P2_1/n$. The asymmetric unit included the cationic complex **1**, two tetraphenylborate ions as counteranions, and three EtOAc molecules as co-crystallized solvent molecules. Figure 6 shows the molecular structure of the cationic complex **1**. Compound **1** adopts a similar conformation to those observed in other Ru^{II}(TPA)(diimine) complexes.[26] The tertiary amine nitrogen atom (N1), two pyridyl nitrogen atoms (N3 and N4) of the TPA ligand, and one of the imine nitrogen atoms of the

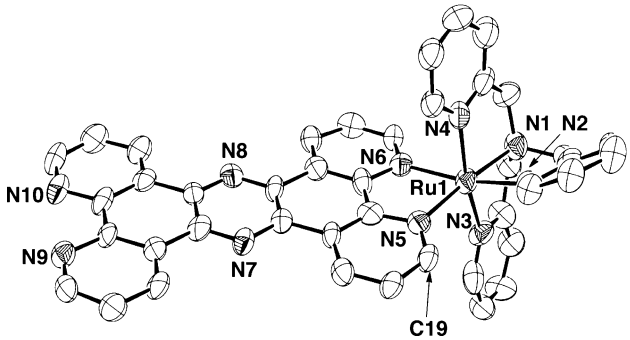

Figure 6. Crystal structure of the cationic part of complex **1**; thermal ellipsoids are set at 50% probability.

© 2013 Wiley-VCH Verlag GmbH & Co. KGaA, Weinheim

tpphz ligand form the equatorial plane and the tpphz ligand and the axial pyridine ring of the TPA ligand were tilted towards the equatorial plane, owing to steric repulsion between them. The dihedral angles between the equatorial coordination plane and the axial pyridine ring and the tpphz ligand were 119.8° and 153.5°, respectively. The interatomic distance between the 6-carbon atom on the axial pyridine ring of the TPA ligand and the C19 carbon atom of the tpphz ligand was 3.33 Å.

Similar distortion, owing to steric repulsion, was also observed in other Ru^{II}(TPA)(diimine) complexes.[26] As a result of the steric repulsion between the tpphz ligand and the axial pyridine ring of the TPA ligand, the Ru–N2 and Ru–N6 bond lengths were elongated compared to those of other Ru–N bonds and the degree of elongation of complex **1** was larger than that for other Ru^{II}(TPA)(diimine) complexes (Table 1).[26] The tpphz ligand was almost planar, even after metal coordination,[28b] and the mean deviation of each atom from the least-square mean plane was 0.031 Å. As a result of the high planarity and the extended π conjugation, the tpphz ligand formed an intermolecular π–π-stacked pair (see the Supporting Information, Figure S8a) and the distance between the two tpphz ligands in the pair was 3.32 Å. The other side of the tpphz ligand formed π–π-stacking interactions with two phenyl rings of the tetraphenylborate counteranion, one of which formed a face-to-face π–π interaction whilst the other formed an edge-to-face π–π interaction (see the Supporting Information, Figure S8b). The distance between the π–π-stacked pair of the tpphz ligands and the phenyl ring of the tetraphenylborate ion was 3.67 Å, whilst that from the edge of the other phenyl ring to the tpphz plane was 3.52 Å.

Table 1. Comparison of bond lengths [Å] and angles [°] in Ru^{II}–TPA–diimine complexes.

diimine	bpy[a]	bpm[a]	phen[a]	tpphz (**1**)
Ru1–N1	2.085(3)	2.093(3)	2.084(2)	2.086(7)
Ru1–N2	2.102(3)	2.101(3)	2.115(2)	2.127(7)
Ru1–N3	2.048(3)	2.068(3)	2.042(3)	2.092(7)
Ru1–N4	2.078(3)	2.091(3)	2.079(2)	2.039(7)
Ru1–N5	2.065(3)	2.086(3)	2.074(3)	2.045(7)
Ru1–N6	2.101(2)	2.092(2)	2.096(2)	2.130(7)
N1-Ru1-N2	79.1(1)	79.9(1)	79.0(1)	79.5(3)
N1-Ru1-N3	83.5(1)	82.6(1)	84.5(1)	80.3(3)
N1-Ru1-N4	80.6(1)	79.8(1)	80.0(1)	83.9(3)
N5-Ru1-N6	77.3(1)	77.8(1)	79.1(1)	79.0(3)
N1-Ru1-N5	175.9(1)	171.7(1)	172.8(1)	174.9(3)
N2-Ru1-N6	167.9(1)	168.8(2)	169.5(1)	165.2(2)
N2-Ru1-N5	100.6(1)	100.4(1)	100.9(1)	98.8(3)

[a] See ref. [26].

Photo- and electrochemical properties: The electronic spectra of complexes **1**, $[\mathbf{1}+H]^+$, **2**, and **3** were recorded in MeCN (Figure 7) and their absorption maxima are summarized in Table 2, together with those of $[Ru^{II}(bpy)_3]^{2+}$[24a] and $[Ru^{II}(TPA)(bpy)]^{2+}$ for comparison.[26] For all four complexes, the π–π* transitions of the tpphz moieties were observed as doubly peaked bands at about 350–400 nm and the MLCT transitions from the Ru^{II} centers to the tpphz ligands appeared at about 430 nm. The molar coefficients of the MLCT absorption for complex **2** were almost double those for complex **1**, because the MLCT transition from the Ru^{II} center in the $Ru^{II}(bpy)_2$ moiety to the tpphz ligand overlapped that from the Ru^{II} center in the Ru^{II}(TPA) unit. In addition, the MLCT absorption band for complex **3** was slightly weaker than that of complex **1**. The MLCT absorption bands of complexes $[\mathbf{1}+H]^+$, **2**, and **3** were red-shifted relative to that of complex **1**, thus indicating a stabilization of the π* orbitals of the tpphz ligands in complexes $[\mathbf{1}+H]^+$, **2**, and **3** through the ligation of proton or metal ions at the vacant coordination sites of the tpphz ligands.

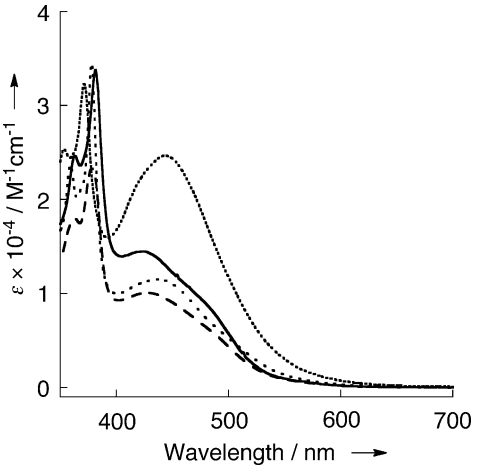

Figure 7. Electronic spectra of complexes **1** (solid line), $[\mathbf{1}+H]^+$ (dashed line), **2** (dotted line), and **3** in MeCN (dotted-spaced line).

In MeCN, complexes **1**, $[\mathbf{1}+H]^+$, **2**, and **3** exhibited relatively weak phosphorescent emissions, which were derived from the relaxation of the triplet MLCT excited states (Figure 8). Other previously reported Ru^{II}(TPA)(diimine) complexes[26] did not display phosphorescence, owing to quenching by the photodissociation reaction of the axial pyridine moiety of the TPA ligand through metal-centered (MC) triplet excited states.[26] The observation of phosphorescence of the Ru^{II}(TPA)(tpphz) complexes indicates that the dissociation pathways of the pyridine moiety through the MC triplet excited states of complexes **1**, $[\mathbf{1}+H]^+$, **2**, and **3** should not be so thermally accessible and, thus, that the triplet MLCT states could be stabilized and relatively emissive. It should be noted that the emissions that were observed for the four complexes were enhanced in CH_2Cl_2 and similar behavior was also observed for the corresponding compound, $[(bpy)_2Ru^{II}(\mu\text{-tpphz})Ru^{II}(bpy)_2]^{4+}$.[37]

The redox potentials of complexes **1**, $[\mathbf{1'}+H]^+$, **2**, and **3** were determined by cyclic and differential-pulse voltammetry (CV and DPV, respectively) at room temperature in MeCN solution that contained tetrabutylammonium hexafluorophosphate ($(n\text{Bu})_4NPF_6$) as a supporting electrolyte under an Ar atmosphere (see the Supporting Information, Figure S10). The electrochemical data are summarized in

 © 2013 Wiley-VCH Verlag GmbH & Co. KGaA, Weinheim

Table 2. Spectroscopic data in MeCN and CH_2Cl_2.

	Absorption		Emission		
	MeCN	CH_2Cl_2	MeCN	CH_2Cl_2	PrCN[c]
	λ_{max} [nm] (ε [$\times10^{-3}$ M^{-1}cm^{-1}])		λ_{max} [nm] (λ_{irr} [nm])		
$[Ru(bpy)_3]^{2+}$[a]	451 (14.1), 386 (4.6)		607 (450)		
$[Ru(bpy)(TPA)]^{2+}$[b]	453		–	–	
$[Ru(bpm)(TPA)]^{2+}$[b]	480		–	–	
$[Ru(phen)(TPA)]^{2+}$[b]	423		–	–	
1	424 (13.4), 381 (34.5), 363 (23.6)	428	514 (424)	467 (424)	595, 550 (400)
$[\mathbf{1}+H]^+$	428 (10.1), 378 (23.2), 363 (18.0)	430	–	490 (424)	607, 571 (405)
2	442 (24.7), 371 (32.3), 353 (25.3)	442	615 (442)	591 (442)	516 (400)
3	437 (11.5), 378 (34.5), 359 (23.7)	485	–	569 (485)	629 (430)
1′	433 (sh, 6.9)				537 (425)
$[\mathbf{1'}+H]^+$	408 (sh, 9.5)				532, 516 (420)
2′	437 (21.6)				534 (440)
3′	405 (sh, 6.6)				543 (450)
$[(bpy)_2Ru(\mu\text{-tpphz})Ru(bpy)_2]^{4+}$[a]	442 (36.1), 370 (34.6), 351 (28.1)		671 (443)		

[a] See ref. [28c]. [b] See ref. [26b]. [c] Phosphorescence spectra were recorded in *n*-butyronitrile (PrCN) at −196 °C (see the Supporting Information, Figure S9).

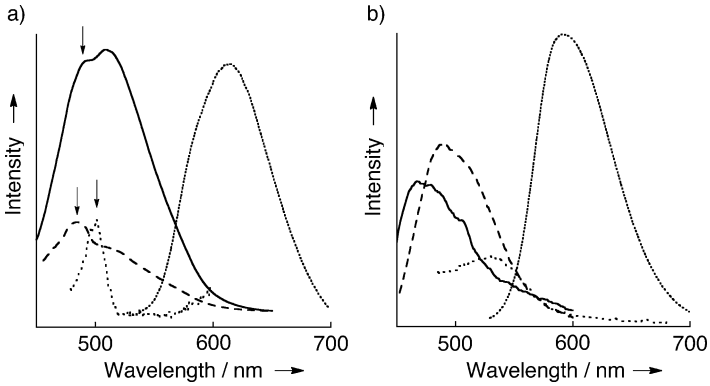

Figure 8. Emission spectra of complexes **1** (solid line), $[\mathbf{1}+H]^+$ (dashed line), **2** (dotted line), and **3** (dotted-spaced line) in MeCN (a) and CH_2Cl_2 (b). The emissions indicated by arrows were derived from the Raman diffraction of the incident light. The wavelengths of the incident light are $\lambda = 424$ nm for complex **1**, 424 nm for complex $[\mathbf{1}+H]^+$, 442 nm for complex **2**, and 485 nm for complex **3**.

Table 3. The redox potentials that were assigned to the $Ru^{II/III}$ redox couples for the Ru^{II}(TPA) units were almost identical for all four complexes (+1.07 V versus SCE) and the redox waves were pseudo-reversible. These results indicate that protonation and metal coordination at the vacant diimine site of the tpphz ligand do not perturb the characteristics of the Ru^{II}(TPA) unit on the other rim of the tpphz ligand. Complex **2** showed another oxidation wave at +1.31 V versus SCE, which should be derived from the $Ru^{II/III}$ redox couple for the Ru center in the $Ru^{II}(bpy)_2$ moiety. This conclusion is consistent with the results of the DFT calculations, as described above. On the other hand, the reduction waves of the tpphz ligand ($tpphz^{0/1-}$) were positively shifted by protonation and metal coordination at the vacant diimine site of the tpphz ligand and the redox potentials increased in the order: **1** (−0.97 V) < $[\mathbf{1}+H]^+$ (−0.95 V) < **3** (−0.93 V) < **2** (−0.87 V). This trend can be accounted for by the stabilization of the π* orbital of the tpphz ligand through protonation and metal coordination (see above).

Thermal dissociation reactions: The thermal dissociation of the axial pyridylmethyl arms in complexes **1**, $[\mathbf{1}+H]^+$, **2**, and **3** were investigated by ^{1}H NMR spectroscopy in $[D_3]$MeCN. When solutions of these complexes were heated at 80 °C in $[D_3]$MeCN, the intensity of the methylene signals of the TPA ligands gradually decreased and, instead, another set of signals appeared in relatively upfield regions (Figure 9) for all four complexes. These new signals contained an AB quartet pair (J = 16.2 Hz) and a singlet in the range $\delta = 3$–5 ppm, all of which were derived from the methylene protons of the TPA ligand. As described in previous reports,[26] the spectroscopic changes that were observed in the ^{1}H NMR spectra could be ascribed to the thermal dissociation of the axial pyridylmethyl moiety of the TPA ligand to give partially dissociated complexes **1′**, $[\mathbf{1'}+H]^+$, **2′**, and **3′** (Figure 9, open form), accompanied by a structural change to afford a facially tridentate TPA ligand with one uncoordinated pyridylmethyl arm. The upfield-shifted singlet signal was derived from the

Table 3. Redox potentials (V versus SCE) of Ru^{II}–tpphz complexes **1**–**3**, $[(bpy)_2Ru(tpphz)]^{2+}$ and $[(\mu\text{-tpphz})\{Ru(bpy)_2\}_2]^{4+}$ as references.[28b]

Compound	$tpphz^{0/1-}$	Ru^{II}/Ru^{III}
1	−0.97	+1.06
$[\mathbf{1}+H]^+$	−0.95	+1.07
2	−0.87	+1.07/+1.31
3	−0.93	+1.08
$[(bpy)_2Ru(tpphz)]^{2+}$[b]	−0.87	+1.33
$[(bpy)_2Ru(\mu\text{-tpphz})Ru(bpy)_2]^{4+}$[b]	−0.71	+1.34

[a] Potentials were determined by differential pulse voltammetry in MeCN in the presence of 0.1 M $(n\text{Bu})_4NPF_6$ as the supporting electrolyte under a N_2 atmosphere at RT. [b] See ref. [28b].

© 2013 Wiley-VCH Verlag GmbH & Co. KGaA, Weinheim

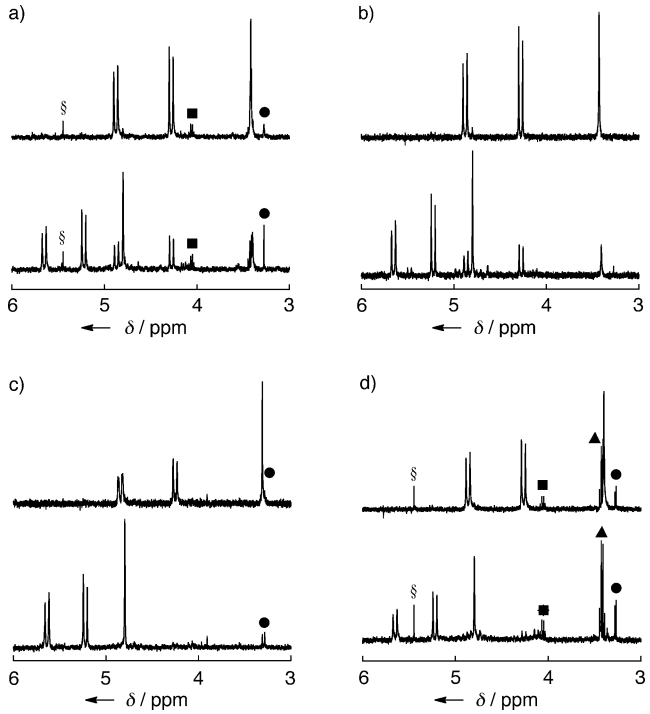

Figure 9. ^{1}H NMR spectroscopic changes upon photoirradiation of complexes **1** (a), [**1**+H]$^+$ (b), **2** (c), and **3** in [D$_3$]MeCN (d). Concentration: 1.7 mM (a), 1.6 mM (b), 1.3 mM (c), 1.7 mM (d). Top: ^{1}H NMR spectra of the open form; bottom: ^{1}H NMR spectra after photoirradiation at 420 nm for 10 h. § CH_2Cl_2, ■ EtOAc, ▲ Et_2O, ● MeOH.

methylene protons of the dissociated pyridylmethyl moiety.[26] For further confirmation of the formation of the "open-form" complexes with accompanying axial MeCN ligands that were derived from the solvent, we performed MS (ESI-TOF) analysis of the four products that were obtained from the thermal reactions of complexes **1**, [**1**+H]$^+$, **2**, and **3** in MeCN. The observed peak clusters in the spectra were in good agreement with those that were expected for the corresponding MeCN-coordinated species in light of the *m*/*z* values and isotopic patterns (Figure 10). In addition, the product of the thermal reaction of complex **1** in MeCN gave a ^{1}H NMR signal at $\delta = 2.16$ ppm in [D$_3$]MeCN, which was ascribed to the coordinated MeCN ligand (see the Supporting Information, Figure S11). The ^{1}H NMR signal showed a slight downfield shift (by $\Delta\delta = 0.20$ ppm) compared to that of free MeCN, owing to coordination to the Ru^{II} center.

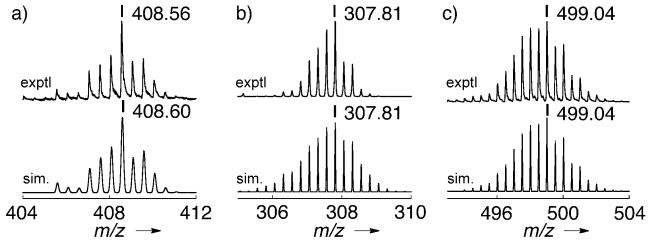

Figure 10. MS (ESI-TOF) of complexes **1′** (a), **2′** (b), and **3′** in MeCN (c). Top: experimental results; bottom: simulated spectra.

Kinetic analysis of the thermal dissociation reactions of the axial pyridine moiety was performed to investigate the reaction mechanisms (Table 4). The first-order rate constants of the reactions at various temperatures were determined in MeCN by monitoring the absorbance changes at 440 nm for each complex (see the Experimental Section). The obtained rate constants were plotted against the inverse of the temperature to provide an Eyring plot (see the Supporting Information, Figure S12).[38] The activation parameters of the reaction, activation enthalpy ($\Delta H^{\neq}$), and activation entropy ($\Delta S^{\neq}$) were determined by linear analysis.

Table 4. First-order rate constants (k) [$\times 10^{-5}$ s^{-1}] and activation parameters for the thermal structural changes of complexes **1**, [**1**+H]$^+$, **2**, and **3** in [D$_3$]MeCN.

	1	[**1**+H]$^+$	**2**	**3**
k (332 K)	1.0	0.90	0.72	0.99
k (335 K)	1.5	1.3	1.0	1.3
k (338 K)	1.8	1.8	1.8	1.4
k (341 K)	2.6	2.0	1.9	2.4
k (344 K)	3.4	2.8	2.6	2.9
$\Delta H^{\neq}$ [kJ mol^{-1}]	92	77	95	82
$\Delta S^{\neq}$ [J mol^{-1} K^{-1}]	−64	−111	−57	−94

The activation parameters of the four complexes investigated herein were very similar to one another (Table 4), thus indicating that their thermal dissociation reactions all proceeded through the same mechanism. The large, negative $\Delta S^{\neq}$ values indicate that the transition state involves strong MeCN coordination to the Ru^{II} center (see below) through an interchange-associative (I_a) mechanism (see the Supporting Information, Figure S13).[39] The positive $\Delta H^{\neq}$ values also indicate that the seven-coordinate Ru^{II} complex is thermodynamically unstable as a transition state.[33]

Photoinduced recoordination of the dissociated pyridine: The photoinduced recoordination reactions of the dissociated pyridine moieties in complexes **1′**, [**1′**+H]$^+$, **2′**, and **3′** were investigated by using NMR spectroscopy (Figure 9) under photoirradiation at 430 nm. On the photoirradiation of a solution of complex **1′** in [D$_3$]MeCN, the ^{1}H NMR signals for the methylene TPA protons in the dissociated species gradually diminished, whilst the signals for closed-form complex **1** gradually became more intense. After 4 h, the spectroscopic changes ceased, thus indicating that the reaction mixture had reached a photostationary state, and the integral ratio between complexes **1** and **1′** was 2:1 (Figure 9a, bottom), that is, 67% conversion from complex **1′** into complex **1**. The photoirradiation of a solution of protonated complex [**1′**+H]$^+$ also afforded a photostationary state between complexes [**1**+H]$^+$ and [**1′**+H]$^+$. However, in comparison to neutral complex **1**, the conversion from the open form into the closed form was much improved, thus exhibiting an integral ratio of [**1**+H]$^+$/[**1′**+H]$^+$ = 5:1 (Figure 9b, bottom), that is, 83% conversion from complex [**1′**+H]$^+$ into [**1**+H]$^+$. In sharp contrast, it should be noted that the photoirradiation of solutions of dinuclear complexes **2′** and

 © 2013 Wiley-VCH Verlag GmbH & Co. KGaA, Weinheim

3′ for 10 h led to complete conversion into closed-form species **2** and **3**, without the presence of any remaining complexes **2′** and **3′**, respectively (Figure 9c,d, bottom). Similar behavior was also observed in the photochemical reactions of closed-form complexes **1** and $[\mathbf{1}+H]^+$ in $[D_3]$MeCN, thus giving rise to a photostationary state that included the corresponding open-form complex (**1′** or $[\mathbf{1}'+H]^+$). In sharp contrast, no spectroscopic changes were observed during the course of the photoirradiation of solutions of complexes **2** and **3** in $[D_3]$MeCN.

To investigate the mechanism of the complete conversion of the open-form dinuclear complexes into their corresponding closed form, we determined the quantum yields (ϕ, at 430 nm) for the photoinduced recoordination of the pyridine moiety in complexes **1′**, $[\mathbf{1}'+H]^+$, **2′**, and **3′** (Table 5). Experiments with $[Fe^{III}(oxalato)_3]^{3-}$ as an actinometer, in accordance with previously reported procedure,[40] allowed us to determine the quantum yields in the photoconversion of complexes **1′**, $[\mathbf{1}'+H]^+$, **2′**, and **3′** to be 0.014, 0.015, 0.024, and 0.013, respectively. Because the quantum yields for the four complexes are not significantly different to one another, the reason for the different conversion efficiencies of these four complexes cannot be the improvement in the quantum yield of the recoordination reactions of the dissociated pyridine moiety relative to those of the corresponding photodissociation reactions. The detailed reaction mechanisms will be discussed below.

Table 5. Quantum yields (ϕ) of the recoordination reactions at $\lambda =$ 430 nm and the photoconversion efficiencies of open-form complexes **1′**–**3′**.

Compound	Quantum yield (ϕ)	Photoconversion efficiency [%] (λ_{irr} [nm])
1′	0.014	67 (430)
$[\mathbf{1}'+H]^+$	0.015	83 (430)
2′	0.024	100 (430)
3′	0.013	100 (430)
$[Ru(bpy)(TPA)]^{2+}$[a]	0.0057	40 (423)
$[Ru(bpm)(TPA)]^{2+}$[a]	0.028	89 (453)
$[Ru(phen)(TPA)]^{2+}$[a]	0.011	65 (423)

[a] See ref. [26b].

Perturbation of the excited states by metal coordination: As mentioned above, the four Ru^{II}–tpphz complexes **1**, $[\mathbf{1}+H]^+$, **2**, and **3** showed thermal dissociation reactions in MeCN, concomitant with their structural transformation into open-form complexes **1′**, $[\mathbf{1}'+H]^+$, **2′**, and **3′**, respectively, in quantitative yield, which contained a free pyridylmethyl moiety on the facial η^3-TPA ligand and an axial MeCN ligand. Thus, in MeCN, the open-form complexes are thermodynamically more stable than the closed-form complexes. This result is consistent with the calculated energy difference between complexes **2** and **2′** as mentioned above.

Under photoirradiation conditions, the open-form complexes turned back into their corresponding closed-form complexes: Complex **1′** afforded a photostationary state with a conversion efficiency of 67% from complex **1′**, protonated complex $[\mathbf{1}+H]^+$ exhibited improved efficiency (83%) from $[\mathbf{1}'+H]^+$, and dinuclear complexes **2** and **3** achieved complete conversion into their corresponding closed-form complexes. To elucidate the controlling factor of the photoinduced conversion efficiency, we focused on the perturbation of the energy level of the triplet MLCT excited states (^{3}MLCT*) by protonation and metal coordination at the vacant site of the tpphz ligand.

It has been proposed that the photodissociation of ligands in Ru^{II} complexes occurs through the triplet MC excited states (^{3}MC*) that are formed by the thermal conversion of ^{3}MLCT* states, which generated through very fast intersystem crossing from the singlet MLCT excited state (^{1}MLCT*).[41] From the resulting ^{3}MC* state, the ligand dissociation proceeds as a thermal process through an unstable coordinate intermediate (Figure 11a).[41] The photodissociation and photorecoordination reactions of Ru^{II}(TPA)(diimine) complexes proceed in the same manner: The axial pyridine moiety in the closed form and the coordinated

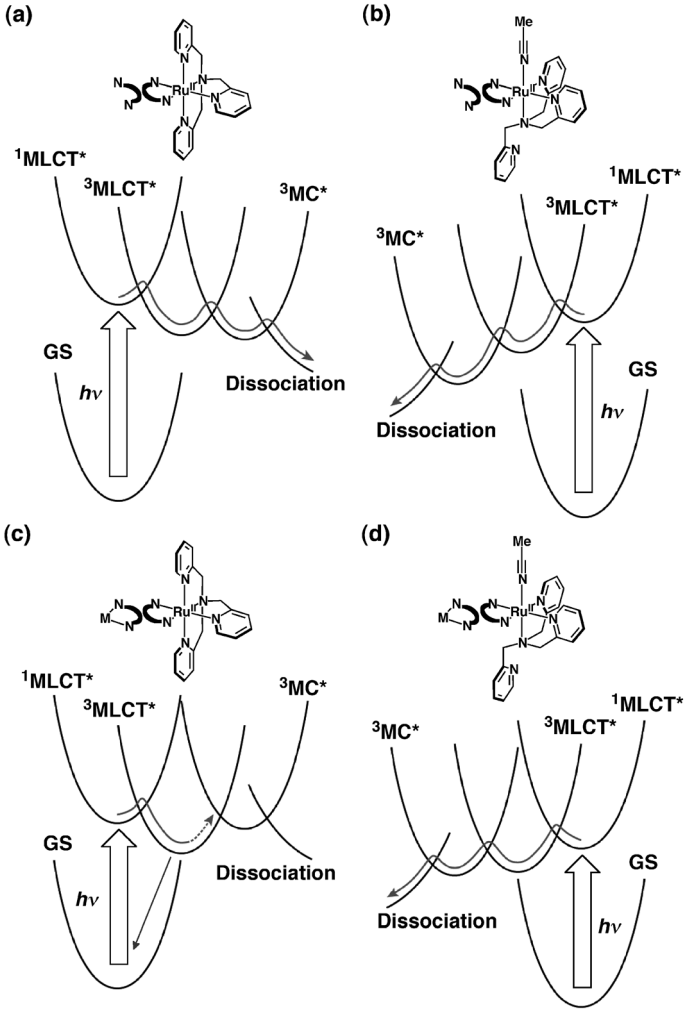

Figure 11. Plausible energy diagrams for the photoinduced dissociation and recoordination reactions of Ru^{II}(TPA)(tpphz) complexes **1** (a), **1′** (b), **2** or **3** (c), and **2′** or **3′** (d). GS denotes the ground state.

 © 2013 Wiley-VCH Verlag GmbH & Co. KGaA, Weinheim

MeCN molecule in the open form dissociate through their corresponding ^{3}MC* states. Based on the UV/Vis and emission spectra of complexes, **1**, [**1**+H]$^+$, **2**, and **3**, the ^{1}MLCT* and ^{3}MLCT* states are stabilized by protonation or metal coordination at the vacant diimine site of the tpphz ligand that is bound to the Ru^{II}(TPA) unit. The cause of the bathochromic shifts of the MLCT absorption and the emission maxima is stabilization of the LUMO (π^*) orbital that is localized on the tpphz ligand by protonation or metal coordination.[42]

The stabilization of the π^* orbital of the tpphz ligand was also confirmed by electrochemical studies, in which the reduction potential of the tpphz ligand was positively shifted in the order: **2**>**3**>[**1**+H]$^+$>**1** (see above). However, protonation and metal coordination at the vacant site of the tpphz ligand probably do not affect the ^{3}MC* state of the Ru^{II} center in the Ru^{II}(TPA) unit, judging from the identical oxidation potentials of the Ru$^{II/III}$ redox couples for the units in all four complexes. Therefore, in the closed forms, which contain the tetradentate TPA ligand, the transition process from the ^{3}MLCT* state into the ^{3}MC* state can be perturbed by protonation and metal coordination at the vacant site of the tpphz ligand when the ^{3}MLCT* state is well-stabilized relative to the ^{3}MC* state (Figure 11c). As a result, the activation barrier ($\Delta G_1^{\ddagger}$) of the thermal transition from the ^{3}MLCT* state into the ^{3}MC state becomes large enough not to be overcome at the reaction temperature (Figure 12, lower black line). On the other hand, the ^{3}MC* states of the open-form complexes are highly stabilized in comparison with those in the closed-form complexes, because the Ru^{II} centers are weakly coordinated by a MeCN molecule instead of a strong pyridine ring of the TPA ligand (Figure 11b,d).[43] As a consequence, the ^{3}MC* state is at a lower energy than the ^{3}MLCT* state in the MeCN-bound open-form complexes, even after the ^{3}MLCT* state is stabilized by protonation or metal coordination at the vacant site of the tpphz ligand (Figure 11d). Therefore, the activation barrier of the thermal transition from the ^{3}MLCT* state into the ^{3}MC state remains low enough to promote the dissociation reaction of the MeCN ligand at the reaction temperature.

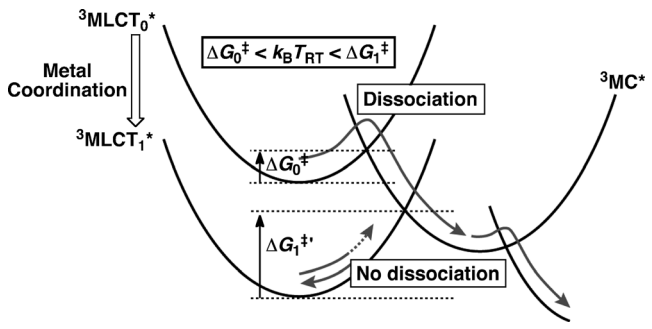

Figure 12. Schematic representation of the stabilization of a ^{3}MLCT* state by metal coordination to the ligand and the resulting disturbance of the transition into the MC* state.

Conclusion

We have achieved the completely photochromic structural conversion between the closed and open forms of dinuclear [{Ru^{II}(TPA)}(μ-tpphz)(ML)] complexes (ML = Ru^{II}(bpy)$_2$, Pd^{II}Cl$_2$), thus demonstrating molecular bistability. Heating a solution of the closed-form complex in MeCN quantitatively afforded the corresponding open-form complex, which contained a coordinated MeCN ligand and a facial η^3-TPA ligand, with an uncoordinated pyridylmethyl arm. On the contrary, illumination of the solution induced the complete conversion of the partially dissociated (open-form) complex that was obtained from the thermal process into the original fully coordinated (closed-form) complex. This reversible structural conversion between two states of a transition-metal complex has been accomplished by a simple perturbation of the electronic structure of the complex, that is, further metal coordination to the other coordination site of the π-conjugated bis-diimine ligand of the complex. Metal coordination to the opposite site of the bis-diimine ligand causes a lowering of the energy level of the LUMO (π^*) orbital of the ligand, which results in the stabilization of the ^{3}MLCT* state of the complex. In the closed form, the stabilization of the ^{3}MLCT* state hinders the transition into the ^{3}MC* state, which is the key excited state in the photoinduced ligand dissociation and recoordination, whereas the ^{3}MC* state in the closed form is originally stabilized by the substitution of one pyridine ligand for a MeCN solvent molecule and, thus, the transition from the ^{3}MLCT* to ^{3}MC* is still possible, even after further metal coordination.

The strategy presented in the work is applicable to the development of the complete regulation of molecular functionality by external stimuli on the basis of molecular bistability. This kind of unique molecular machinery, which is completely controlled by thermal and photonic stimuli, is highly promising for future applications in photoresponsive drug-delivery systems[44] or on/off switchable catalysts.[45,46]

Experimental Section

Materials and synthesis: 5,6-Diamino-1,10-phenanthroline (phendiamine),[31] [RuCl(TPA)]$_2$(ClO$_4$)$_2$,[35] and [RuCl$_2$(bpy)$_2$]·2H$_2$O[32] (bpy = 2,2′-bipyridine) were prepared according to literature procedures. 1,10-Phenanthroline-5,6-dione (phendione) was synthesized according to a literature procedure[30] and purified by column chromatography on silica gel (Wakogel C-200, 75–150 μm; CHCl$_3$/MeOH, 10:1 v/v).

Methods: NMR measurements were performed on JEOL EX270 and Bruker AVANCE400 spectrometers. UV/Vis absorption spectra were recorded in MeCN on a Shimazu UV-3600 spectrophotometer at RT. Emission spectra were recorded on JASCO FP-6500 and HITACHI F-4500 spectrofluorometers at RT. MS (ESI-TOF) was performed on Applied Biosystems QSTAR Pulsar i and JEOL JMS-T100CS mass spectrometers. Photoirradiation of the sample was performed by using a Xe light source (300 W) on an ASAHI SPECTRA MAX-301.

[Ru^{II}(TPA)(phendione)](PF$_6$)$_2$: Orange solid [Ru^{II}Cl(TPA)]$_2$(ClO$_4$)$_2$[35] (0.432 g, 0.41 mmol) was added to a degassed solution of phendione[30] (0.450 g, 2.1 mmol) in MeOH (50 mL) under an Ar atmosphere. The mixture was heated at reflux overnight and then cooled to RT. NH_4PF_6 was added to the solution to give a brown precipitate. The precipitate was fil-

 © 2013 Wiley-VCH Verlag GmbH & Co. KGaA, Weinheim

tered, thoroughly washed with Et_2O, and then dried under vacuum. Yield: 0.551 g (0.62 mmol, 75%); ^{1}H NMR (CD_3CN): δ = 9.86 (dd, J = 5.4, 0.7 Hz, 1H; phen-H2), 9.26 (dd, J = 5.4, 1.3 Hz, 1H; phen-H9), 9.08 (d, J = 5.8 Hz, 1H; pyr-H6(ax)), 8.71 (dd, J = 7.9, 1.2 Hz, 1H; phen-H4), 8.42 (dd, J = 7.9, 1.2 Hz, 1H; phen-H7), 8.18 (dd, J = 6.2, 2.1 Hz, 1H; phen-H3), 7.80 (dd, J = 5.6, 0.7 Hz, 2H; pyr-H6(eq)), 7.74–7.70 (m, 3H; pyr-H4(ax) and pyr-H4(eq)), 7.67 (dt, J = 7.8, 1.5 Hz, 1H; phen-8H), 7.41 (d, J = 7.9 Hz, 3H; pyr-H3(ax) and pyr-H3(eq)), 7.34 (dt, J = 6.7, 1.4 Hz, 1H; pyr-H5(ax)), 7.05 (t, J = 6.5 Hz, 2H; pyr-H5(eq)), 5.50 and 5.17 (ABq, J = 17.1 Hz, 4H; CH_2(eq)), 4.75 ppm (s, 2H; CH_2(ax)); MS (ESI): m/z calcd: 301.05 $[M-2PF_6]^{2+}$; found: 301.06; elemental analysis calcd (%) for $C_{30}H_{24}N_6O_2P_2F_{12}Ru$: C 40.41, H 2.71, N 9.43; found: C 40.70, H 2.90, N 9.70.

$[Ru^{II}(TPA)(tpphz)](PF_6)_2$ (1): Brown solid $[Ru^{II}(TPA)(phendione)](PF_6)_2$ (0.199 g, 0.22 mmol) was added to a degassed solution of phendiamine[31] (0.100 g, 0.48 mmol) in MeOH (60 mL) under an Ar atmosphere. The mixture was heated at reflux for 12 h and then cooled to RT. The solution was filtered through Celite 535 and thoroughly washed with MeCN. NH_4PF_6 and water were added to the concentrated filtrate to afford a precipitate. The orange product was filtered, thoroughly washed with water, EtOAc, and Et_2O, and dried under vacuum. Yield: 0.172 g (0.16 mmol, 73%); ^{1}H NMR (CD_3CN, 1.7 mM): δ = 10.14 (d, J = 5.6 Hz, 1H; tpphz(*h*)-H6), 9.75–9.70 (m, tpphz(*h*)-H4, 3H; tpphz(*j*)-H6 and pyr-H6(ax)), 9.62 (d, J = 7.8 Hz, 1H; tpphz(*c*)-H6), 9.56 (d, J = 5.6 Hz, 1H; tpphz(*a*)-H4), 9.32 (d, J = 6.1 Hz, 1H; tpphz(*a*)-H6), 8.98 (dd, J = 4.5, 1.7 Hz, 1H; tpphz(*j*)-H4), 8.85 (dd, J = 4.5, 1.7 Hz, 1H; pyr-H5(ax)), 8.43 (dd, J = 8.1, 2.7 Hz, 1H; tpphz(*h*)-H5), 8.02 (dd, J = 8.1, 2.8 Hz, 1H; tpphz(*c*)-H4), 7.96 (d, J = 5.0 Hz, 2H; pyr-H6(eq)), 7.92–7.85 (m, 2H; pyr-H4(ax) and tpphz(*j*)-H5), 7.78 (t, J = 8.4 Hz, 1H; tpphz(*c*)-H5), 7.62 (dt, J = 7.7, 1.7 Hz, 2H; pyr-H4(eq)), 7.48–7.42 (m, 4H; pyr-H3(ax), pyr-H3(eq), and tpphz(*a*)-H5), 6.96 (t, J = 6.1 Hz, 2H; pyr-H5(eq)), 5.72 and 5.28 (ABq, J = 17.1 Hz, 4H; CH_2(eq)), 4.85 ppm (s, 2H; CH_2(ax)); UV/Vis (MeCN): λ_{max} ($\log\varepsilon$) = 363 ($\pi\rightarrow\pi^*$, 4.37), 381 ($\pi\rightarrow\pi^*$, 4.54), 424 nm (MLCT, 4.13); MS (ESI): m/z calcd: 388.08 $[M-2PF_6]^{2+}$; found: 388.10; elemental analysis calcd (%) for $C_{42}H_{30}N_{10}P_2F_{12}Ru{\cdot}0.5H_2O$: C 46.94, H 2.91, N 13.03; found: C 46.97, H 3.19, N 13.12.

$[Ru(\eta^3\text{-}TPA)(tpphz)(MeCN)(PF_6)_2$ (1′): A solution of complex **1** (10 mg, 9.4 μmol) in MeCN (5 mL) was heated at 60°C for 5 days in the dark. EtOAc was added to this solution to afford a precipitate. The orange precipitate was filtered, thoroughly washed with EtOAc and Et_2O, and dried under vacuum. Yield: 8 mg (7 μmol, 70%); ^{1}H NMR (CD_3CN, 1.7 mM): δ = 9.79 (dd, J = 8.1, 1.5 Hz, 2H; tpphz(*h*)-H6 and tpphz(*j*)-H6), 9.71 (d, J = 8.3 Hz, 2H; tpphz(*h*)-H4 and tpphz(*j*)-H4), 9.11 (d, J = 5.3 Hz, 2H; tpphz(*a*)-H6 and tpphz(*c*)-H6), 9.01(d, J=3.2 Hz, 2H; pyr-H6(eq)), 8.79 (dd, J = 5.3, 1.2 Hz, 2H; tpphz(*a*)-H4 and tpphz(*c*)-H4), 8.44 (d, J = 4.0 Hz, 1H; pyr-H6(ax)), 8.08 (dd, J = 8.2, 5.3 Hz, 2H; tpphz(*h*)-H5 and tpphz(*j*)-H5), 7.96–7.90 (m, 4H; pyr-H4(eq), tpphz(*a*)-H5, and tpphz(*c*)-H5), 7.54–7.46 (m, 5H; pyr-H4(ax), pyr-H5(eq), and pyr-H3(eq)), 7.18 (dd, J = 6.8, 4.9 Hz, 1H; pyr-H5(ax)), 7.02 (d, J = 7.8 Hz, 1H; pyr-H3(ax)), 4.88 and 4.28 (ABq, J = 17.1 Hz, 2H; CH_2(eq)), 3.42 (s, 1H; CH_2(ax)), 2.16 ppm (s, 3H; MeCN); UV/Vis (MeCN): λ_{max} ($\log\varepsilon$) = 433 nm (MLCT, 3.84); MS (ESI): m/z calcd: 408.60 $[M-2PF_6]^{2+}$; found: 408.56.

$[Ru(TPA)(tpphz\text{-}H^+)](PF_6)_3$ ([1+H]$^+$): Trifluoromethanesulfonic acid (8 μL, 0.09 mmol) was added to a solution of complex **1** (0.031 g, 0.029 mmol) in MeCN (20 mL). The solution was filtered through Celite 535 and thoroughly washed with MeCN. NH_4PF_6 and water were added to the concentrated filtrate to afford a precipitate. The orange product was filtered, thoroughly washed with water, and dried under vacuum. Yield: 0.021 g (0.017 mmol, 59%); ^{1}H NMR (CD_3CN, 1.6 mM): δ = 10.17–10.12 (m, 2H; tpphz(*h*)-H6 and pyr-H6(ax)), 10.07 (dd, J = 8.2, 1.5 Hz, 1H; tpphz(*h*)-H4), 9.99 (dd, J = 8.2, 1.2 Hz, 1H; tpphz(*j*)-H6), 9.78 (dd, J = 8.1, 0.8 Hz, 1H; tpphz(*c*)-H6), 9.58 (dd, J = 5.4, 1.1 Hz, 1H; tpphz(*a*)-H6), 9.30–9.21 (m, 3H; tpphz(*a*)-H4, tpphz(*j*)-H4, and pyr-H5(ax)), 8.51 (dd, J = 8.1, 5.5 Hz, 1H; tpphz(*h*)-H5), 8.29–8.21 (m, 2H; tpphz(*j*)-H5 and pyr-H4(ax)), 8.07 (dd, J = 7.1, 5.4 Hz, 1H; tpphz(*c*)-H4), 7.81 (dd, J = 5.8, 0.8 Hz, 2H; pyr-H6(eq)), 7.76 (dt, J = 7.7, 1.3 Hz, 1H; tpphz(*a*)-H5), 7.61 (dt, J = 7.7, 1.5 Hz, 2H; pyr-H4(eq)), 7.45–7.37 (m, 4H; pyr-H3(ax), pyr-H3(eq), and tpphz(*c*)-H5), 6.92 (t, J = 6.1 Hz, 2H; pyr-H5(eq)), 5.65 and 5.23 (ABq, J = 17.1 Hz, 4H; CH_2(eq)), 4.80 ppm (s, 2H; CH_2(ax)); UV/Vis (MeCN): λ_{max} ($\log\varepsilon$) = 363 ($\pi\rightarrow\pi^*$, 4.26), 378 ($\pi\rightarrow\pi^*$, 4.37), 428 nm (MLCT, 4.00); elemental analysis calcd (%) for $C_{42}H_{31}N_{10}P_3F_{18}Ru{\cdot}H_2O{\cdot}0.5$ MeCN: C 41.31, H 2.78, N 11.76; found: C 41.48, H 3.06, N 11.56.

$[Ru(\eta^3\text{-}TPA)(tpphz\text{-}H^+)(MeCN)(PF_6)_3$ ([1′+H]$^+$): A solution of complex [**1**+H]$^+$ (12 mg, 0.010 mmol) in MeCN (5 mL) was heated at 60°C for 5 days in the dark. EtOAc was added to the solution to afford a precipitate. The orange precipitate was filtered, thoroughly washed with EtOAc and Et_2O, and dried under vacuum. Yield: 9 mg (7 μmol, 70%); ^{1}H NMR (CD_3CN, 1.6 mM): δ = 9.77 (dd, J = 8.1, 1.6 Hz, 2H; tpphz(*h*)-H6 and tpphz(*j*)-H6), 9.66 (d, J = 8.0 Hz, 2H; tpphz(*h*)-H4 and tpphz(*j*)-H4), 9.12 (d, J = 5.5 Hz, 2H; tpphz(*a*)-H6 and tpphz(*c*)-H6), 8.95 (d, J = 3.6 Hz, 2H; pyr-H6(eq)), 8.79 (dd, J = 5.3, 1.2 Hz, 2H; tpphz(*a*)-H4 and tpphz(*c*)-H4), 8.44 (d, J = 4.8 Hz, 1H; pyr-H6(ax)), 8.07 (dd, J = 8.2, 5.3 Hz, 2H; tpphz(*h*)-H5 and tpphz(*j*)-H5), 7.95–7.90 (m, 4H; pyr-H4, tpphz(*a*)-H5, and tpphz(*c*)-H5), 7.52–7.46 (m, 5H; pyr-H4(ax), pyr-H5(eq), and pyr-H3(eq)), 7.18 (dd, J = 7.6, 4.9 Hz, 1H; pyr-H5(ax)), 7.04 (d, J = 7.8 Hz, 1H; pyr-H3(ax)), 4.88 and 4.28 (ABq, J = 16.9 Hz, 2H; CH_2(eq)), 3.43 (s, 1H; CH_2(ax)), 2.16 ppm (s, 3H; MeCN); UV/Vis (MeCN): λ_{max} ($\log\varepsilon$) = 408 nm (MLCT, 3.98).

$[(bpy)_2Ru(\mu\text{-}tpphz)Ru(TPA)](PF_6)_4$ (2): A solution of $[RuCl_2(bpy)_2]{\cdot}2H_2O$[32] (96 mg, 0.19 mmol) and silver trifluoromethanesulfonate (98 mg, 0.38 mmol) in acetone (30 mL) was heated at 40°C for 8 h and then cooled to RT. After filtration to remove the resulting silver chloride and washing the solid with acetone (10 mL), the solution of complex **1** (82.3 mg, 0.077 mmol) in acetone (20 mL) was added to the collected filtrate. Then, the mixture was degassed and stirred for 3 days under an Ar at RT. The solution was filtered, NH_4PF_6 and water were added, and the mixture was stored at 4°C for 2 h until a red precipitate appeared. The precipitate was filtered off, washed with water, EtOH, and Et_2O, and dried under vacuum. Yield: 110 mg (0.062 mmol, 80%). ^{1}H NMR (CD_3CN, 1.3 mM): δ = 10.56 (d, J = 4.5 Hz, 1H; tpphz(*h*)-H6), 10.34 (d, J = 7.2 Hz, 1H; tpphz(*h*)-H4), 10.24 (d, J = 7.0 Hz, 1H; tpphz(*j*)-H6), 10.14–10.04 (m, 2H; tpphz(*j*)-H4 and pyr-H6(ax)), 9.64 (d, J = 7.3 Hz, 1H; tpphz(*c*)-H6), 8.92–8.85 (m, 5H; pyr-H5(ax), pyr′-H6(ax), and pyr′-H6(eq)), 8.72–8.63 (m, 3H; tpphz(*h*)-H5 and pyr′-H3(eq)), 8.33–8.05 (m, 12H; pyr-3H(ax), pyr-4H(ax), pyr-H6(eq), pyr′-H5(ax), pyr′-H3(ax), pyr′-H4(eq), tpphz(*c*)-H4, and tpphz(*j*)-H5), 7.87 (t, J = 7.7 Hz, 1H; tpphz(*a*)-H6), 7.77–7.60 (m, 8H; pyr-H5(eq), pyr-H3(eq), pyr′-H4(ax), tpphz(*a*)-H5, and tpphz(*a*)-H4), 7.52 (t, J = 6.0 Hz, 1H; tpphz(*c*)-H5), 7.42 (t, J = 5.9 Hz, 2H; pyr′-H5(eq)), 7.05 (t, J = 6.1 Hz, 2H; pyr-H4(eq)), 6.12 and 5.59 (ABq, J = 17.5 Hz, 4H; CH_2(eq)), 5.18 ppm (s, 2H; CH_2(ax)); UV/Vis (MeCN): λ_{max} ($\log\varepsilon$) = 353 ($\pi\rightarrow\pi^*$, 4.40), 371 ($\pi\rightarrow\pi^*$, 4.51), 442 nm (MLCT, 4.39); MS (ESI): m/z calcd: 297.55 $[M-4PF_6]^{4+}$; found: 297.59; elemental analysis calcd (%) for $C_{62}H_{46}N_{14}P_4F_{24}Ru_2{\cdot}2H_2O$: C 41.25, H 2.79, N 10.86; found: C 41.10, H 2.85, N 10.77.

$[(bpy)_2Ru(\mu\text{-}tpphz)Ru(\eta^3\text{-}TPA)(MeCN)(PF_6)_4$ (2′): A solution of complex **2** (20 mg, 0.011 mmol) in MeCN (5 mL) was heated at 60°C for 5 days in the dark. EtOAc was added to this solution to form a precipitate. The orange precipitate was filtered, thoroughly washed with EtOAc and Et_2O, and dried under vacuum. Yield: 15 mg (8.3 μmol, 75%); ^{1}H NMR (CD_3CN, 1.3 mM): δ = 10.03 (d, J = 5.3 Hz, 2H; tpphz(*h*)-H6 and tpphz(*j*)-H6), 9.99 (dd, J = 8.3, 1.2 Hz, 2H; tpphz(*a*)-H6 and tpphz(*c*)-H6), 9.06 (d, J = 5.4 Hz, 2H; pyr-H6(eq)), 8.84 (dd, J = 5.4, 1.2 Hz, 2H; pyr′-H6(ax)), 8.58 (d, J = 8.1 Hz, 2H; pyr′-H6(eq)), 8.54 (d, J = 8.2 Hz, 2H; tpphz(*h*)-H4 and tpphz(*j*)-H4), 8.44 (d, J = 4.8 Hz, 1H; pyr-H6(ax)), 8.30 (dd, J = 5.3, 1.2 Hz, 2H; tpphz(*a*)-H4 and tpphz(*c*)-H4), 8.18–8.12 (m, 4H; tpphz(*h*)-H5 and tpphz(*j*)-H5), 8.05–8.00 (m, 4H; pyr′-H4(ax) and pyr′-H4(eq)), 7.93–7.87 (m, 4H; pyr-H4(eq), tpphz(*a*)-H5, and tpphz(*c*)-H5), 7.74 (d, J = 5.5 Hz, 2H; pyr′-H3(ax) and pyr′-H3(eq)), 7.56 (dt, J = 7.8, 1.8 Hz, 1H; pyr-H4(ax)), 7.51–7.44 (m, 6H; pyr-H5(eq), pyr′-H5(ax) and pyr′-H5(eq)), 7.28–7.20 (m, 3H; pyr-H5(ax), pyr-H3(eq)), 6.96 (d, J = 7.8 Hz, 1H; pyr-H3(ax)), 4.85 and 4.25 (ABq, J = 17.1 Hz, 2H; CH_2(eq)), 3.31 (s, 2H; CH_2(ax)), 2.16 ppm (s, 3H; MeCN); UV/Vis (MeCN): λ_{max} ($\log\varepsilon$) = 437 nm (MLCT, 4.33); MS (ESI): m/z calcd: 307.81 $[M-4PF_6]^{4+}$; found: 307.81.

 © 2013 Wiley-VCH Verlag GmbH & Co. KGaA, Weinheim

$[Cl_2Pd(\mu\text{-tpphz})Ru(TPA)](PF_6)_2$ (3): A solution of complex **1** (42 mg, 0.040 mmol) and $PdCl_2$ (41 mg, 0.29 mmol) in EtOH (25 mL) was degassed and heated at reflux for 24 h under an Ar atmosphere. Then, the solution was cooled to RT and the solvent was removed under vacuum. The residual brown solid was dissolved in MeCN and the black precipitate was filtered off. The volatile compounds in the orange filtrate were removed and the residue was dissolved in a small amount of DMSO. The solution was filtered, NH_4PF_6 and water were added, and the mixture was stored at 4°C for 2 h until a red precipitate appeared. The precipitate was filtered off, washed with water, EtOH, and Et_2O, and dried under vacuum. Yield: 21 mg (0.017 mmol, 43%); ^{1}H NMR (CD_3CN, 1.5 mM): $\delta = 10.32$ (d, $J = 5.1$ Hz, 1H; tpphz(*h*)-H6), 9.98 (d, $J = 8.2$ Hz, 1H; tpphz(*h*)-H4), 9.70 (d, $J = 8.1$ Hz, 1H; tpphz(*j*)-H6), 9.64 (d, $J = 5.3$ Hz, 1H; tpphz(*a*)-H6), 9.59–9.56 (m, 2H; tpphz(*c*)-H6 and pyr-H6(ax)), 9.30 (d, $J = 5.3$ Hz, 1H; tpphz(*a*)-H4), 9.11–9.06 (m, 2H; tpphz(*j*)-H4 and pyr-H5(ax)), 7.91 (d, $J = 5.0$ Hz, 2H; pyr-H6(eq)), 7.76 (t, $J = 7.0$ Hz, 1H; tpphz(*a*)-H5), 7.58 (dt, $J = 7.8$, 1.5 Hz, 2H; pyr-H4(eq)), 7.46–7.38 (m, 4H; tpphz(*c*)-H3, pyr-H3(ax), and pyr-H3(eq)), 6.89 (t, $J = 6.3$ Hz, 2H; pyr-H5(eq)), 5.66 and 5.22 (ABq, $J = 17.0$ Hz, 4H; CH_2(eq)), 4.80 ppm (s, 2H; CH_2(ax)); UV/Vis (MeCN): λ_{max} ($\log\varepsilon$) = 359 ($\pi\rightarrow\pi^*$, 4.37), 378 ($\pi\rightarrow\pi^*$, 4.54), 437 nm (MLCT, 4.06); MS (ESI): *m*/*z* calcd: 476.51 $[M-2PF_6]^{2+}$; found: 476.49; elemental analysis calcd (%) for $C_{42}H_{30}N_{10}P_2F_{12}Cl_2RuPd$: C 38.89, H 2.80, N 10.80; found: C 39.19, H 2.50, N 10.88.

$[Cl_2Pd(\mu\text{-tpphz})Ru(\eta^3\text{-TPA})(MeCN)](PF_6)_2$ (3′): A solution of complex **3** (12 mg, 9.7 μmol) in MeCN (5 mL) was heated at 60°C for 5 days in the dark. EtOAc was added to this solution to afford a precipitate. The orange precipitate was filtered, thoroughly washed with EtOAc and Et_2O, and dried under vacuum. Yield: 8 mg (6 μmol, 62%); ^{1}H NMR (CD_3CN, 1.7 mM): $\delta = 9.99$ (dd, $J = 4.2$, 1.2 Hz, 2H; tpphz(*h*)-H6 and tpphz(*j*)-H6), 9.64 (dd, $J = 8.2$, 1.3 Hz, 2H; tpphz(*h*)-H4 and tpphz(*j*)-H4), 9.23 (dd, $J = 5.4$, 1.3 Hz, 2H; tpphz(*a*)-H6 and tpphz(*c*)-H6), 9.10 (d, $J = 5.2$ Hz, 2H; tpphz(*a*)-H4 and tpphz(*j*)-H4), 8.89 (dd, $J = 5.3$, 1.3 Hz, 2H; pyr-H6(eq)), 8.47 (dd, $J = 4.8$, 1.0 Hz, 1H; pyr-H6(ax)), 8.24–8.18 (m, 4H; pyr-H4(eq), tpphz(*h*)-H5, and tpphz(*j*)-H5), 7.91 (dt, $J = 7.9$, 1.5 Hz, 2H; tpphz(*a*)-H5 and tpphz(*c*)-H5), 7.56 (dt, $J = 7.8$, 1.8 Hz, 1H; pyr-H4(ax)), 7.52–7.54 (m, 4H; pyr-H3(eq) and pyr-H5(eq)), 7.22 (m, 1H; pyr-H5(ax)), 7.04 (d, $J = 7.9$ Hz, 1H; pyr-H3(eq)), 4.87 and 4.27 (ABq, $J = 17.0$ Hz, 4H; CH_2(eq)), 3.40 (s, 2H; CH_2(ax)), 2.15 ppm (s, 3H; MeCN); UV/Vis (MeCN): λ_{max} ($\log\varepsilon$) = 405 nm (MLCT, 3.82); MS (ESI): *m*/*z* calcd: 499.04 $[M-2PF_6]^{2+}$; found: 499.04.

Electrochemical measurements: Cyclic and differential-pulse voltammetry were performed in MeCN in the presence of 0.1 M $[(n\text{-butyl})_4N]PF_6$ ($TBAPF_6$) as an electrolyte under an Ar atmosphere at RT, with a Pt disk as a working electrode, $Ag/AgNO_3$ as a reference electrode, and Pt wire as an auxiliary electrode.

Photoirradiation: The photoirradiation of complexes **1**, $[\mathbf{1}+H]^+$, **2**, and **3** was performed by using a Xe light source (300 W) on an ASAHI SPECTRA MAX-301 that was equipped with a band-path filter for a bandwidth-at-half-maximum of 20 nm, centered at 430 nm. The complexes were dissolved in freshly distilled MeCN to a concentration of 3.4×10^{-5} M for the UV/Vis measurements and in $[D_3]$MeCN to a concentration of 1.6 mM for the ^{1}H NMR experiments. The sample solutions were degassed by bubbling with Ar. The degassed solutions were irradiated at 430 nm for 12 h and the reaction was monitored by monitoring the absorption or ^{1}H NMR spectroscopic changes.

Determination of quantum yields: The quantum yields of the photodissociation reactions of complexes **1**, $[\mathbf{1}+H]^+$, **2**, and **3** were determined by using standard methods on an actinometer (potassium ferrioxalate) in water with photoirradiation at 430 nm.[40] The reaction was monitored to observe the decrease in absorbance at 430 nm over time. The data for the initial stage, during which a linear change was observed, were used to determine the quantum yield.[47]

Kinetics analysis of the thermal processes: The absorbance change at 440 nm was monitored and fit to Equation (1).

$$A = A_\infty + (A_0 - A_\infty)\, e^{-kt} \quad (1)$$

Determination of rate constants by using ^{1}H NMR spectroscopy. The concentration of the starting complex at each time was determined as the integral ratio between the signal of the equatorial methylene moieties of the TPA ligand and that of the methyl groups of tetraethylsilane, which was used as an internal standard. The decrease in concentration of the starting complex was plotted against the time and the plot was fitted to Equation (2).

$$c = c_0 e^{-kt} \quad (2)$$

Similar experiments were performed at various temperatures and the obtained rate constants were plotted against the reciprocal of the temperature. The resulting plot was fitted to the Eyring equation (Equation (3)) to estimate the activation parameters.

$$\ln(kT^{-1}) = -\Delta H^{\ddagger} R^{-1} T^{-1} + \Delta S^{\ddagger} R^{-1} + \ln(\chi k_B/h) \quad (3)$$

X-ray crystallography of complex 1: A single crystal of complex **1** was obtained by recrystallization through the slow diffusion of benzene into its solution in acetone in the presence of excess sodium tetraphenylborate to exchange the counteranion for improved crystallinity. The diffraction data were measured on a Rigaku Mercury CCD system at the Photon Factory–Advanced Ring for Pulse X-rays (PF-AR NW2A) of the High Energy Accelerator Research Organization (KEK). The data were integrated, scaled, and corrected for absorption by using the HKL2000 program. The structure was solved by using direct methods (SIR-97) and expanded with differential Fourier techniques. All non-hydrogen atoms were refined anisotropically and the refinement was performed by using full-matrix least-squares on *F*. All calculations were performed by using the Yadokari-XG crystallographic software package.[48]

Crystallographic data. $C_{42}H_{30}N_{10}Ru\cdot2B(C_6H_5)_4\cdot3C_4H_8O_2$; $M_w = 904.40$; red-orange crystals; monoclinic; space group $P2_1/n$; $a = 14.3387(7)$, $b = 17.8504(8)$, $c = 33.121(2)$ Å; $\beta = 95.39(2)°$; $V = 8439.9(8)$ Å^3; $Z = 4$; $\rho_{calcd} = 1.321$ g cm^{-3}; $F_{000} = 3512$; $R1 = 0.1071$ ($I > 2\sigma(I)$), $wR2 = 0.3066$ (all data); GOF = 0.984. CCDC-921694 (**1**) contains the supplementary crystallographic data for this paper. These data can be obtained free of charge from The Cambridge Crystallographic Data Centre via www.ccdc.cam.ac.uk/data_request/cif.

Computational methods: The structures of complexes **2** and **2′** were optimized by using the hybrid (Hartree–Fock/DFT) B3LYP functional.[49] The SDD basis set[50] were used for Ru atoms and the D95** basis set[51] for H, C, and N atoms. The program that we used was the Gaussian 09 package.[52] A model structure of complex **2** was developed on the basis of the crystal structures of $[Ru^{II}(TPA)(1,10\text{-phenanthroline})](PF_6)_2$[26] and *cis*-$[Ru^{II}Cl_2(bpy)_2]$.[32]

Acknowledgements

This work was supported by Grants-in-Aid (20108010, 21350035, 24245011) from the Japan Society for the Promotion of Science (JSPS), a grant through a specially promoted area "Photochromism" (21021013) from the Ministry of Education, Science and Technology of Japan (MEXT), and a grant from The Asahi Glass Foundation.

[1] a) V. Balzani, A. Credi, M. Venturi, *Molecular Devices and Machines*, Wiley-VCH, Weinheim, **2003**; b) V. Balzani, A. Credi, F. M. Raymo, J. F. Stoddart, *Angew. Chem.* **2000**, *112*, 3484–3530; *Angew. Chem. Int. Ed.* **2000**, *39*, 3348–3391; c) K. Kinbara, T. Aida, *Chem. Rev.* **2005**, *105*, 1377–1400; d) W. R. Browne, B. L. Feringa, *Nat. Nanotechnol.* **2006**, *1*, 25–35.

[2] a) A. Bissell, E. Córdova, A. E. Kaifer, J. F. Stoddart, *Nature* **1994**, *369*, 133–137; b) J. D. Badjic, V. Balzani, A. Credi, S. Silvi, J. F. Stoddart, *Science* **2004**, *303*, 1845–1849.

[3] a) J.-P. Collin, C. Dietrich-Buchecker, P. Gavina, M. C. Jimenez-Molero, J.-P. Sauvage, *Acc. Chem. Res.* **2001**, *34*, 477–487; b) M. C.

 © 2013 Wiley-VCH Verlag GmbH & Co. KGaA, Weinheim

Jiménez, C. Dietrich-Buchecker, J.-P. Sauvage, *Angew. Chem.* **2000**, *112*, 3422–3425; *Angew. Chem. Int. Ed.* **2000**, *39*, 3284–3287; c) M. C. Jimenez-Molero, C. Dietrich-Buchecker, J.-P. Sauvage, *Chem. Eur. J.* **2002**, *8*, 1456–1466; d) M. C. Jimenez-Molero, C. Dietrich-Buchecker, J.-P. Sauvage, *Chem. Commun.* **2003**, 1613–1616.

[4] G. S. Kottas, L. I. Clarke, D. Horinek, J. Michl, *Chem. Rev.* **2005**, *105*, 1281–1376.

[5] a) N. Koumura, R. W. J. Zijlstra, R. A. van Delden, N. Harada, B. L. Feringa, *Nature* **1999**, *401*, 152–154; b) B. L. Feringa, *Acc. Chem. Res.* **2001**, *34*, 504–513; c) J. Wang, B. L. Feringa, *Science* **2011**, *331*, 1429–1432.

[6] a) D. A. Leigh, J. K. Y. Wong, F. Dehez, F. Zerbetto, *Nature* **2003**, *424*, 174–179; b) J. V. Hernandez, E. R. Kay, D. A. Leigh, *Science* **2004**, *306*, 1532–1537; c) E. R. Kay, D. A. Leigh, F. Zerbetto, *Angew. Chem.* **2007**, *119*, 72–196; *Angew. Chem. Int. Ed.* **2007**, *46*, 72–191.

[7] a) T. R. Kelly, M. C. Bowyer, K. V. Bhaskar, D. Bebbington, A. Garcia, F. Lang, M. H. Kim, M. P. Jette, *J. Am. Chem. Soc.* **1994**, *116*, 3657–3658; b) T. R. Kelly, I. Tellitu, J. P. Sestelo, *Angew. Chem.* **1997**, *109*, 1969–1972; *Angew. Chem. Int. Ed. Engl.* **1997**, *36*, 1866–1868; c) A. P. Davis, *Angew. Chem.* **1998**, *110*, 953–954; *Angew. Chem. Int. Ed.* **1998**, *37*, 909–910; d) T. R. Kelly, H. De Silva, R. A. Silva, *Nature* **1999**, *401*, 150–152; e) T. R. Kelly, R. A. Silva, H. De Silva, S. Jasmin, Y. Zhao, *J. Am. Chem. Soc.* **2000**, *122*, 6935–6949; f) C. Manzano, W.-H. Soe, H. S. Wong, F. Ample, A. Gourdon, N. Chandrasekhar, C. Joachim, *Nat. Mater.* **2009**, *8*, 576–579; g) S. Pekker, E. Kovats, G. Oszlanyi, G. Benyei, G. Klupp, G. Bortel, I. Jalsovszky, E. Jakab, F. Borondics, K. Kamaras, M. Bokor, G. Kriza, K. Tompa, G. Faigel, *Nat. Mater.* **2005**, *4*, 764–767.

[8] a) T. Muraoka, K. Kinbara, Y. Kobayashi, T. Aida, *J. Am. Chem. Soc.* **2003**, *125*, 5612–5613; b) T. Muraoka, K. Kinbara, T. Aida, *Nature* **2006**, *440*, 512–515.

[9] a) I. Rayment, W. R. Rypniewski, K. Schmidt-Baese, R. Smith, D. R. Tomchick, M. M. Benning, D. A. Winkelmann, G. Wesenberg, H. M. Holden, *Science* **1993**, *261*, 50–58; b) I. Rayment, H. M. Holden, M. Whittaker, C. B. Yohn, M. Lorenz, K. C. Holmese, R. A. Milligan, *Science* **1993**, *261*, 58–65.

[10] a) D. Stock, A. G. W. Leslie, J. E. Walker, *Science* **1999**, *286*, 1700–1705; b) R. I. Menz, J. E. Walker, A. G. W. Leslie, *Cell* **2001**, *106*, 331–341.

[11] a) P. Bodis, M. R. Panman, B. H. Bakker, A. Mateo-Alonso, M. Prato, W. J. Buma, A. M. Brouwer, E. R. Kay, D. A. Leigh, S. Woutersen, *Acc. Chem. Res.* **2009**, *42*, 1462–1469; b) S. Bonnet, J.-P. Collin, *Chem. Soc. Rev.* **2008**, *37*, 1207–1217; c) S. Saha, J. F. Stoddart, *Chem. Soc. Rev.* **2007**, *36*, 77–92.

[12] a) K.-W. Cheng, C.-C. Lai, P.-T. Chiang, S.-H. Chiu, *Chem. Commun.* **2006**, 2854–2856; b) T. Ooya, D. Inoue, H. S. Choi, Y. Kobayashi, S. Loethen, D. H. Thompson, Y. H. Ko, K. Kim, N. Yui, *Org. Lett.* **2006**, *8*, 3159–3162; c) C.-K. Koo, B. Lam, S.-K. Leung, M. H.-W. Lam, W.-Y. Wong, *J. Am. Chem. Soc.* **2006**, *128*, 16434–16435.

[13] S. Saha, A. H. Flood, J. F. Stoddart, S. Impellizzeri, S. Silvi, M. Venturi, A. Credi, *J. Am. Chem. Soc.* **2007**, *129*, 12159–12171.

[14] a) C. P. Collier, G. Mattersteig, E. W. Wong, Y. Luo, K. Beverly, J. Sampaio, F. M. Raymo, J. F. Stoddart, J. R. Heath, *Science* **2000**, *289*, 1172–1175; b) C. P. Collier, J. O. Jeppesen, Y. Luo, J. Perkins, E. W. Wong, J. R. Heath, J. F. Stoddart, *J. Am. Chem. Soc.* **2001**, *123*, 12632–12641; c) V. Balzani, M. Clemente-León, A. Credi, B. Ferrer, M. Venturi, A. H. Flood, J. F. Stoddart, *Proc. Natl. Acad. Sci. USA* **2006**, *103*, 1178–1183.

[15] a) S. Silvi, A. Arduini, A. Pochini, A. Secchi, M. Tomasulo, F. M. Raymo, M. Baroncini, A. Credi, *J. Am. Chem. Soc.* **2007**, *129*, 13378–13379; b) H. Wu, D. Zhang, L. Su, K. Ohkubo, C. Zhang, S. Yin, L. Mao, Z. Shuai, S. Fukuzumi, D. Zhu, *J. Am. Chem. Soc.* **2007**, *129*, 6839–6846; c) V. Serreli, C.-F. Lee, E. R. Kay, D. A. Leigh, *Nature* **2007**, *445*, 523–527.

[16] a) P. Thordarson, E. J. A. Bijsterveld, A. E. Rowan, R. J. M. Nolte, *Nature* **2003**, *424*, 915–918; b) C. Monnereau, P. Hidalgo Ramos, A. B. C. Deutman, J. A. A. W. Elemans, R. J. M. Nolte, A. E. Rowan, *J. Am. Chem. Soc.* **2010**, *132*, 1529–1531; c) M. von Delius, E. M. Geertsema, D. A. Leigh, D.-T. D. Tang, *J. Am. Chem. Soc.* **2010**, *132*, 16134–16145.

[17] a) S. Shinkai, T. Nakaji, Y. Nishida, T. Ogawa, O. Manabe, *J. Am. Chem. Soc.* **1980**, *102*, 5860–5865; b) S. Shinkai, T. Nakaji, T. Ogawa, K. Shigematsu, O. Manabe, *J. Am. Chem. Soc.* **1981**, *103*, 111–115.

[18] a) K. Ichimura, S.-K. Oh, M. Nakagawa, *Science* **2000**, *288*, 1624–1626; b) Y. Yu, M. Nakano, T. Ikeda, *Nature* **2003**, *425*, 145.

[19] a) M. V. Peters, R. Goddard, S. Hecht, *J. Org. Chem.* **2006**, *71*, 7846–7849; b) M. V. Peters, R. S. Stoll, A. Kühn, S. Hecht, *Angew. Chem.* **2008**, *120*, 6056–6060; *Angew. Chem. Int. Ed.* **2008**, *47*, 5968–5972; c) R. S. Stoll, M. V. Peters, A. Kuhn, S. Heiles, R. Goddard, M. Bühl, C. M. Thiele, S. Hecht, *J. Am. Chem. Soc.* **2009**, *131*, 357–367.

[20] a) D. Ishii, K. Kinbara, Y. Ishida, N. Ishii, M. Okochi, M. Yohda, T. Aida, *Nature* **2003**, *423*, 628–632; b) A. Bernardos, E. Aznar, M. D. Marcos, R. Martínez-Máñez, F. Sancenón, J. Soto, J. M. Barat, P. Amorós, *Angew. Chem.* **2009**, *121*, 5998–6001; *Angew. Chem. Int. Ed.* **2009**, *48*, 5884–5887.

[21] L. Fabbrizzi, M. Licchelli, P. Pallavicini, L. Parodi, *Angew. Chem.* **1998**, *110*, 838–841; *Angew. Chem. Int. Ed.* **1998**, *37*, 800–802.

[22] a) C. Lodeiro, A. J. Parola, F. Pina, C. Bazzicalupi, A. Bencini, A. Bianchi, C. Giorgi, A. Masotti, B. Valtancoli, *Inorg. Chem.* **2001**, *40*, 2968–2975; b) P. Pallavicini, G. Dacarro, C. Mangano, S. Patroni, A. Taglietti, R. Zanoni, *Eur. J. Inorg. Chem.* **2006**, 4649–4657.

[23] a) L. Zelikovich, J. Libman, A. Shanzer, *Nature* **1995**, *374*, 790–792; b) L. Fabbrizzi, F. Gatti, P. Pallavicini, E. Zambarbieri, *Chem. Eur. J.* **1999**, *5*, 682–690.

[24] a) B. Durham, V. J. Caspar, J. K. Nagle, T. J. Meyer, *J. Am. Chem. Soc.* **1982**, *104*, 4803–4810; b) B. Durham, S. R. Wilson, D. J. Hodgson, T. J. Meyer, *J. Am. Chem. Soc.* **1980**, *102*, 600–607; c) S. Bonnet, J.-P. Collin, J.-P. Sauvage, E. Schofield, *Inorg. Chem.* **2004**, *43*, 8346–8354.

[25] S. Venkataramani, U. Jana, M. Dommaschk, F. D. Sönnichsen, F. Tuczek, R. Herges, *Science* **2011**, *331*, 445–448.

[26] a) T. Kojima, T. Sakamoto, Y. Matsuda, *Inorg. Chem.* **2004**, *43*, 2243–2245; b) T. Kojima, T. Morimoto, T. Sakamoto, S. Miyazaki, S. Fukuzumi, *Chem. Eur. J.* **2008**, *14*, 8904–8915.

[27] S. Miyazaki, T. Kojima, S. Fukuzumi, *J. Am. Chem. Soc.* **2008**, *130*, 1556–1557.

[28] a) R. Knapp, A. Schott, M. Rehahn, *Macromolecules* **1996**, *29*, 478–480; b) J. Bolger, A. Gourdon, E. Ishow, J.-P. Launay, *Inorg. Chem.* **1996**, *35*, 2937–2944; c) G. Pourtois, D. Beljonne, C. Moucheron, S. Schumm, A. Kirsch-De Mesmaeker, R. Lazzaroni, J.-L. Bredas, *J. Am. Chem. Soc.* **2004**, *126*, 683–692.

[29] S. Rau, B. Schäfer, D. Gleich, E. Anders, M. Rudolph, M. Friedrich, H. Görls, W. Henry, J. G. Vos, *Angew. Chem.* **2006**, *118*, 6361–6364; *Angew. Chem. Int. Ed.* **2006**, *45*, 6215–6218.

[30] M. Yamada, Y. Tanaka, Y. Yoshimoto, S. Kuroda, I. Shimao, *Bull. Chem. Soc. Jpn.* **1992**, *65*, 1006–1011.

[31] S. Bodige, F. M. MacDonnell, *Tetrahedron Lett.* **1997**, *38*, 8159–8160.

[32] B. P. Sullivan, D. J. Salmon, T. J. Meyer, *Inorg. Chem.* **1978**, *17*, 3334–3341.

[33] T. Ishizuka, T. Sawaki, S. Miyazaki, M. Kawano, Y. Shiota, K. Yoshizawa, S. Fukuzumi, T. Kojima, *Chem. Eur. J.* **2011**, *17*, 6652–6662.

[34] a) S. Tschierlei, M. Presselt, C. Kuhnt, A. Yartsev, T. Pascher, V. Sundstroem, M. Karnahl, M. Schwalbe, B. Schaefer, S. Rau, M. Schmitt, B. Dietzek, J. Popp, *Chem. Eur. J.* **2009**, *15*, 7678–7688; b) S. Tschierlei, M. Karnahl, M. Presselt, B. Dietzek, J. Guthmuller, L. Gonzalez, M. Schmitt, S. Rau, J. Popp, *Angew. Chem.* **2010**, *122*, 4073–4076; *Angew. Chem. Int. Ed.* **2010**, *49*, 3981–3984.

[35] T. Kojima, T. Amano, Y. Ishii, M. Ohba, Y. Okaue, Y. Matsuda, *Inorg. Chem.* **1998**, *37*, 4076–4085.

[36] a) S. Miyazaki, K. Ohkubo, T. Kojima, S. Fukuzumi, *Angew. Chem.* **2007**, *119*, 923–926; *Angew. Chem. Int. Ed.* **2007**, *46*, 905–908; b) T. Kojima, T. Sakamoto, Y. Matsuda, K. Ohkubo, S. Fukuzumi, *Angew. Chem.* **2003**, *115*, 5101–5104; *Angew. Chem. Int. Ed.* **2003**, *42*, 4951–

 © 2013 Wiley-VCH Verlag GmbH & Co. KGaA, Weinheim

4954; c) S. Miyazaki, T. Kojima, T. Sakamoto, T. Matsumoto, K. Ohkubo, S. Fukuzumi, *Inorg. Chem.* **2008**, *47*, 333–343.
[37] C. Chiorboli, M. A. J. Rodgers, F. Scandola, *J. Am. Chem. Soc.* **2003**, *125*, 483–491.
[38] H. Eyring, *J. Chem. Phys.* **1935**, *3*, 107–115.
[39] a) T. Kojima, S. Miyazaki, K. Hayashi, Y. Shimazaki, F. Tani, Y. Naruta, Y. Matsuda, *Chem. Eur. J.* **2004**, *10*, 6402–6410; b) O. Johansson, L. O. Johannissen, R. Lomoth, *Chem. Eur. J.* **2009**, *15*, 1195–1204.
[40] a) L. J. Heidt, G. W. Tregay, F. A. Middleton, Jr., *J. Phys. Chem.* **1970**, *74*, 1876–1882; b) C. H. Langford, C. A. Houlubor, *Inorg. Chim. Acta* **1981**, *53*, L59–L60.
[41] A. Juris, V. Balzani, F. Barigelletti, S. Campagna, P. Beler, A. von Zelewsky, *Coord. Chem. Rev.* **1988**, *84*, 85.
[42] a) F. D'Souza, M. E. Zandler, G. R. Deviprasad, W. Kutner, *J. Phys. Chem. A* **2000**, *104*, 6887–6893; b) Q.-Y. Zhu, Y. Liu, W. Lu, Y. Zhang, G.-Q. Bian, G.-Y. Niu, J. Dai, *Inorg. Chem.* **2007**, *46*, 10065–10070.
[43] In general, MeCN is a weaker ligand than pyridine in the spectrochemical series. Thus, the MeCN complex affords a smaller ligand field splitting and, hence, a more-stable ^{3}MC* state. See: P. Atkins, T. Overton, J. Rourke, M. Weller, F. Armstrong, *Inorganic Chemistry*, 5th ed., Oxford University Press, Oxford, **2010**, p. 475.
[44] a) A. Jana, K. S. P. Devi, T. K. Maiti, N. D. P. Singh, *J. Am. Chem. Soc.* **2012**, *134*, 7656–7659; b) J. L. Vivero-Escoto, I. I. Slowing, C.-W. Wu, V. S.-Y. Lin, *J. Am. Chem. Soc.* **2009**, *131*, 3462–3463.
[45] T. Kojima, K. Nakayama, K. Ikemura, T. Ogura, S. Fukuzumi, *J. Am. Chem. Soc.* **2011**, *133*, 11692–11700.
[46] a) H. Sugimoto, T. Kimura, S. Inoue, *J. Am. Chem. Soc.* **1999**, *121*, 2325–2326; b) R. Cacciapaglia, S. Di Stefano, L. Mandolini, *J. Am. Chem. Soc.* **2003**, *125*, 2224–2227; c) D. Sud, T. B. Norsten, N. R. Branda, *Angew. Chem.* **2005**, *117*, 2055–2057; *Angew. Chem. Int. Ed.* **2005**, *44*, 2019–2021.
[47] G. Gauglitz in *Photochromism Molecule and Systems*, revised edition (Eds.: H. Dürr, H. Bouas-Laurent), Elsevier, Amsterdam, **2003**, p. 30.
[48] a) K. Wakita, *Yadokari-XG*, *Software for Crystal Structure Analyses*, **2001**; b) C. Kabuto, S. Akine, T. Nemoto, E. Kwon, *Release of Software (Yadokari-XG 2009) for Crystal Structure Analyses, J. Cryst. Soc. Jpn.* **2009**, *51*, 218.
[49] a) A. D. Becke, *Phys. Rev. A* **1988**, *38*, 3098–3100; b) C. Lee, W. Yang, R. G. Parr, *Phys. Rev. B* **1988**, *37*, 785–789; c) A. D. Becke, *J. Chem. Phys.* **1993**, *98*, 5648–5652.
[50] D. Andrae, U. Haeussermann, M. Dolg, H. Stoll, H. Preuss, *Theor. Chem. Acc.* **1990**, *77*, 123–141.
[51] T. H. Dunning, P. J. Hay in *Modern Theoretical Chemistry, Vol. 3* (Ed.: H. F. Schaefer, III, Plenum, New York, **1976**, pp. 1–27.
[52] Gaussian 09, Revision B.01, M. J. Frisch, G. W. Trucks, H. B. Schlegel, G. E. Scuseria, M. A. Robb, J. R. Cheeseman, G. Scalmani, V. Barone, B. Mennucci, G. A. Petersson, H. Nakatsuji, M. Caricato, X. Li, H. P. Hratchian, A. F. Izmaylov, J. Bloino, G. Zheng, J. L. Sonnenberg, M. Hada, M. Ehara, K. Toyota, R. Fukuda, J. Hasegawa, M. Ishida, T. Nakajima, Y. Honda, O. Kitao, H. Nakai, T. Vreven, J. A. Montgomery, Jr., J. E. Peralta, F. Ogliaro, M. Bearpark, J. J. Heyd, E. Brothers, K. N. Kudin, V. N. Staroverov, R. Kobayashi, J. Normand, K. Raghavachari, A. Rendell, J. C. Burant, S. S. Iyengar, J. Tomasi, M. Cossi, N. Rega, J. M. Millam, M. Klene, J. E. Knox, J. B. Cross, V. Bakken, C. Adamo, J. Jaramillo, R. Gomperts, R. E. Stratmann, O. Yazyev, A. J. Austin, R. Cammi, C. Pomelli, J. W. Ochterski, R. L. Martin, K. Morokuma, V. G. Zakrzewski, G. A. Voth, P. Salvador, J. J. Dannenberg, S. Dapprich, A. D. Daniels, Ö. Farkas, J. B. Foresman, J. V. Ortiz, J. Cioslowski, D. J. Fox, Gaussian, Inc., Wallingford CT, **2009**.

Received: February 4, 2013
Revised: March 28, 2013
Published online: May 16, 2013

 © 2013 Wiley-VCH Verlag GmbH & Co. KGaA, Weinheim